Geomorphology 382 (2021) 107693

Contents lists available at ScienceDirect

Geomorphology

journal homepage: www.elsevier.com/locate/geomorph

Geomorphology and surficial geology of the Femmilsjøen area, northern Spitsbergen

Lis Allaart [a,b,*], Anders Schomacker [a], Lena M. Håkansson [b], Wesley R. Farnsworth [c], Skafti Brynjólfsson [d], Andreas Grumstad [a], Sofia E. Kjellman [a]

[a] Department of Geosciences, UiT The Arctic University of Norway, Postboks 6050, Langnes, N-9037 Tromsø, Norway
[b] Department of Arctic Geology, The University Centre in Svalbard (UNIS), P.O. Box 156, N-9171 Longyearbyen, Norway
[c] Nordic Volcanological Center, Institute of Earth Sciences, University of Iceland, Askja, Sturlugata 7, IS-102 Reykjavík, Iceland
[d] The Icelandic Institute of Natural History, Borgum við Norðurslóð, IS-600 Akureyri, Iceland.

ARTICLE INFO

Article history:
Received 6 January 2021
Received in revised form 5 March 2021
Accepted 5 March 2021
Available online 9 March 2021

Keywords:
geomorphological map
northern Svalbard
cold-based ice
hard sub-stratum

ABSTRACT

Climate change is amplified in the Arctic, and establishing baseline data for its current character is important. Here we present a map of the geomorphology of the Femmilsjøen area, Spitsbergen, northern Svalbard. The regional physiography is characterised by a low-relief, high elevation mountain plateau, its high-relief steep slopes, and low-relief coastal lowlands. The results indicate that glaciers were most likely warm-based and erosive in the low terrain, whereas there are signatures of colder, less erosive ice on the plateaus during the Late Weichselian. Our study highlights the ongoing glacial and periglacial morphological processes in an area of hard and weathering-resistant bedrock, situated in northern Svalbard.

© 2021 The Authors. Published by Elsevier B.V. This is an open access article under the CC BY license (http://creativecommons.org/licenses/by/4.0/).

1. Introduction

The high Arctic is sensitive to climate change affecting geomorphological processes, landforms and ecosystems (Åkerman, 2005; Kaufman et al., 2009; Rowland et al., 2011; French, 2018; Berthling et al., 2020). As Arctic air and ocean temperatures rise, a direct response is exhibited in the glacial, periglacial and coastal environments. A warming Arctic is characterised by glacial retreat, exposing more land prone to weathering and re-sedimentation processes (Ballantyne, 2002; Strzelecki et al., 2020). Additionally, in periglacial environments the active layer overlaying the permafrost (i.e., ground that undergoes annual freeze and thaw cycles) thickens, which results in enhanced solifluction (Åkerman, 2005; Biskaborn et al., 2019). Furthermore, coastal regions will likely experience increased instability due to enhanced erosional processes caused by more frequent wave action and thawing of permafrost (Lantuit et al., 2012; Sessford et al., 2015; Nicu et al., 2020).

During the Last Glacial Maximum (LGM), the Svalbard Barents-Sea Ice Sheet covered the archipelago, and ice streamed through the fjords and troughs, extending to the shelf edge (Landvik et al., 1998; Ingólfsson, 2011; Hormes et al., 2013). Since the termination of the Last Glacial and the subsequent retreat of the ice sheet, the landscape of Svalbard has been exposed to subaerial weathering and to erosional and depositional processes (Larsen et al., 2018). Geomorphological maps are useful tools to reconstruct the spatiotemporal pattern of glacial retreat in an area (Chandler et al., 2018). In a changing climate, a geomorphological map can serve as a baseline for monitoring and comparison of future landscape change (Kavan, 2019). Furthermore, mapping enhances the understanding of individual landforms and the links between them, as well as the sedimentary, depositional and erosional processes.

Currently, glaciers and ice caps cover 57% of the Svalbard archipelago (Nuth et al., 2013). Since the onset of the Holocene, the landscape has been and is still modulated by small-scale glacial advance-retreat cycles. Large ice-cored moraines and exposed glacial bedforms are prominent in the terrain, primarily formed by Late Holocene glacier advances (Werner, 1993; van der Meer, 2004; Ingólfsson, 2011). Several of these moraines originate from quasi-periodic dynamic surge advances, not directly related to mass balance (Meier and Post, 1969; Sharp, 1988; Sevestre and Benn, 2015; Lovell and Boston, 2017). The glacial forelands of Svalbard have received a lot of research interest, resulting in maps of glacial landforms, landsystems, and glacial sedimentary processes across Svalbard (e.g., de Geer, 1896; Boulton, 1967; Szczęsny et al., 1989; Huddart and Hambrey, 1996; Hart and Watts, 1997; Bennett et al., 1999; Boulton et al., 1999; Glasser et al., 1999; Bennett et al., 2000; Glasser and Hambrey, 2001; van der Meer, 2004; Larsen et al., 2005; Schomacker and Kjær, 2008; Hanáček et al., 2011; Evans et al., 2012; Ewertowski et al., 2016; Farnsworth et al., 2016; Lønne, 2016; Allaart et al., 2018; Lovell et al., 2018; Aradóttir et al., 2019; Fig. 1). However, significant parts of the non-glacier-covered terrain in Svalbard consist of non-glacial landforms, such as blockfields, alluvial fans, areas with extensive raised marine sediments, sets of beach ridges and colluvial fans covering

* Corresponding author at: Department of Geosciences, UiT The Arctic University of Norway, Postboks 6050, Langnes, N-9037 Tromsø, Norway.
E-mail address: lis.allaart@uit.no (L. Allaart).

https://doi.org/10.1016/j.geomorph.2021.107693
0169-555X/© 2021 The Authors. Published by Elsevier B.V. This is an open access article under the CC BY license (http://creativecommons.org/licenses/by/4.0/).

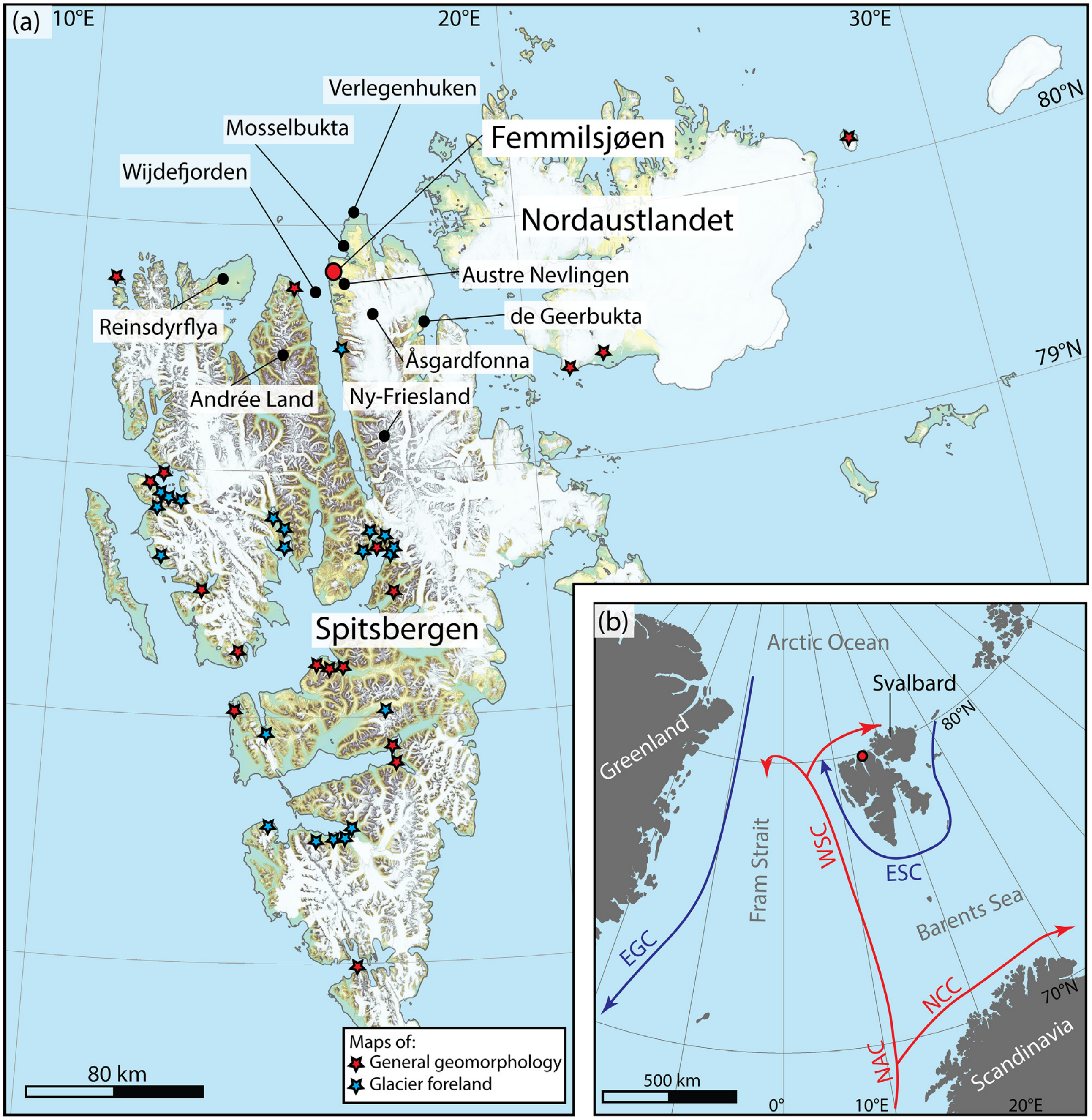

Fig. 1. (a) Overview map of Svalbard, study area marked with a red dot. Red stars indicate locations of published geomorphological maps, blue stars indicate locations of published terrestrial glacier foreland maps (mentioned in the text). The representation of published maps may be slightly biased towards publications in English. (b) Inset map showing the location of Svalbard in the North Atlantic region, warm currents in red (NAC = North Atlantic Current, NCC = North Cape Current and WSC = West Spitsbergen Current), cold currents in blue (ESC = East Spitsbergen Current, EGC = East Greenland Current).

the steeper slopes (e.g., Thompson, 1953; Blake, 1962; Jonsson, 1983; Kristiansen and Sollid, 1986; Tolgensbakk, 1990; Österholm, 1990; Ingólfsson et al., 1995; Ballantyne, 2002; Forman et al., 2004; Lønne and Nemec, 2004; Humlum, 2005; Eckerstorfer et al., 2013; Dallmann, 2015; de Haas et al., 2015; Bourriquen et al., 2018; Fig. 1). High-resolution overview maps of the peri- and paraglacial processes influencing the terrestrial geomorphology exist from southern, central and western Svalbard (e.g., Åkerman and Boardman, 1987; Karczewski et al., 1990; Tolgensbakk et al., 2001; Zwoliński et al., 2013; Rubensdotter et al., 2015a, 2015b; Miccadei et al., 2016; Rubensdotter et al., 2016; Farnsworth et al., 2017; Gjerde et al., 2018; Larsen et al., 2018; Lyså et al., 2018; Rouyet et al., 2019; Berthling et al., 2020; Fig. 1). Studies and geomorphological maps focusing on coastal processes exist from central and northern Svalbard (e.g., Brückner and Schellman, 2003; Sessford et al., 2015; Bourriquen et al., 2018), and a highly detailed geomorphological map of an alluvial fan system exists from central Spitsbergen (Tomczyk et al., 2019; Fig. 1). Geomorphological studies and mapped areas tend to cluster around research stations or settlements, where the landscape can be relatively easily accessed.

To our knowledge, few high-resolution geomorphological maps exist from northern Svalbard and of areas with very subtle to absent glacial imprints – i.e., forelands of suggestively cold-based glaciers (Fig. 1). Furthermore, a geomorphological and surficial geologic map provides a baseline map for future comparison of landscape change. Therefore, we aim to identify processes of deposition and erosion, and describe and discuss morphological characteristics and surficial deposits of the Femmilsjøen area. We do this through geomorphological and surficial geologic mapping based on aerial image interpretation as well as field mapping of the terrestrial area surrounding Lake Femmilsjøen and the foreland of Midtsundstadbreen. A conceptual model highlighting past and present processes summarises our findings.

2. Setting

2.1. Study area

The mapped area is situated in northern Spitsbergen, adjacent to the mouth of Wijdefjorden (Fig. 1). The regional physiography consists of a mountain plateau, its steep slopes, and coastal lowlands. The map covers the surroundings of Lake Femmilsjøen (meaning 'the five mile lake' in Norwegian), limited by Wijdefjorden in the west and the outlets of Åsgardfonna (Longstaffbreen and Midtsundstadbreen) in the east, and extends from 15°35′E to 16°10′E and from 79°44′N to 79°50′N (Figs. 1 and 2). Longstaffbreen, terminating in the eastern end of Femmilsjøen, is a surge-type glacier with its latest recorded surge in the 1960s (Liestøl, 1993; Hagen et al., 1993; Fig. 2). Midtsundstadbreen (south of Longstaffbreen) has a lobate shape with a relatively steep front (Fig. 2).

The bedrock is part of the large-scale folding of the Atomfjella Antiform and consists of metasediments and granitic gneisses (*c.* 1750

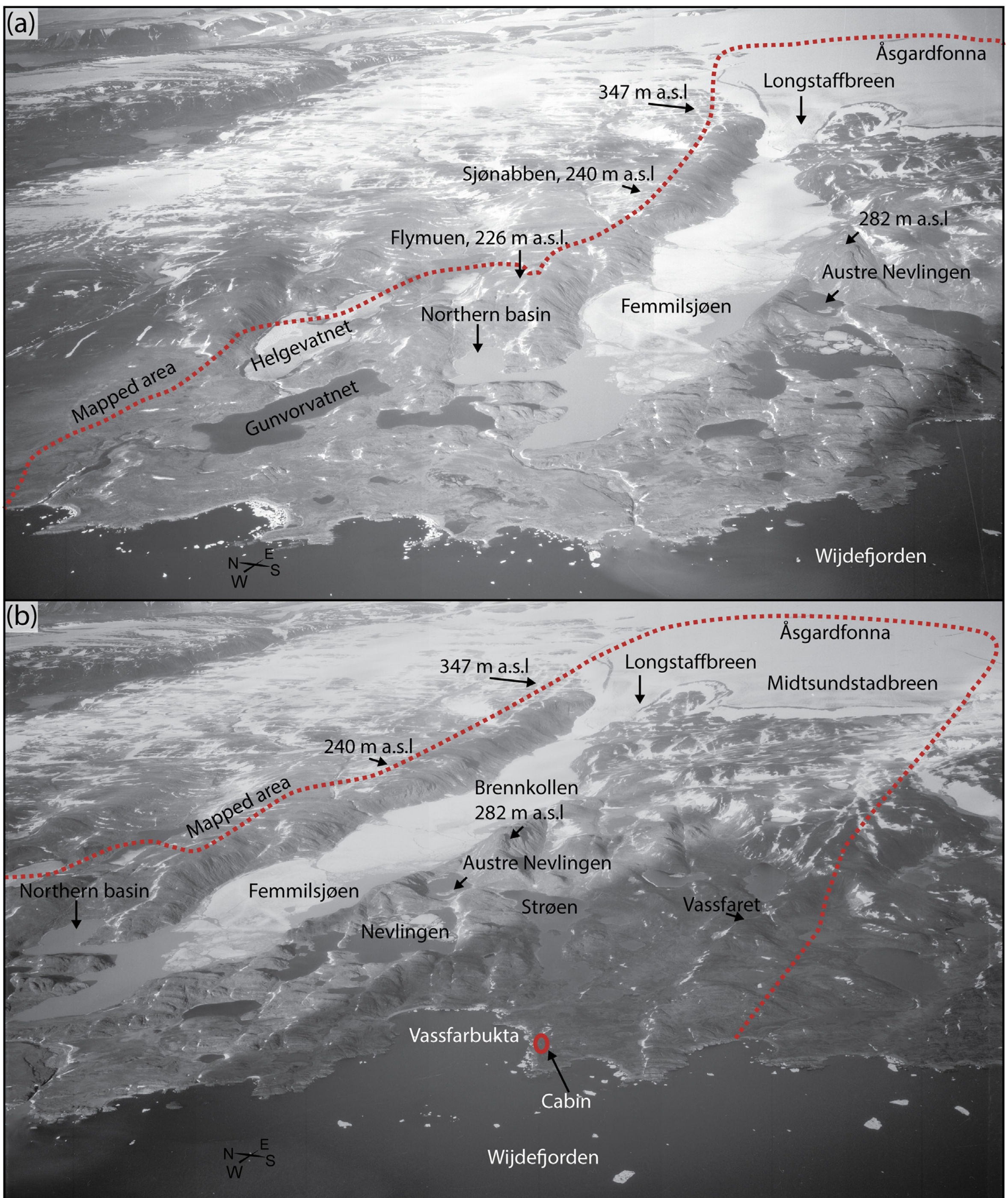

Fig. 2. Two oblique aerial images showing the mapped area. Place names and elevation of the highest peaks in the area are labelled. Aerial images © Norwegian Polar Institute, 1936.

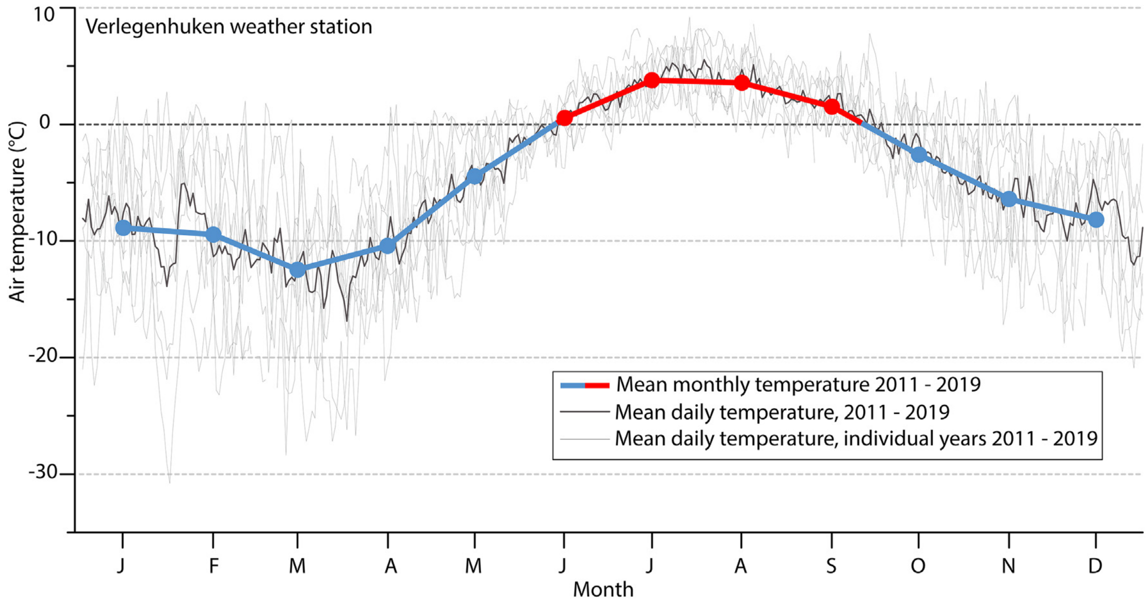

Fig. 3. Mean air temperatures (2011–2019 CE) from the weather station at Verlegenhuken, ~25 km north of the study area. Interannual air temperature variations are larger in winter compared to summer (see Fig. 1 for location; MET Norway, 2020).

Ma; Witt-Nilsson et al., 1998; Dallmann, 2015). Around Femmilsjøen, the Vassfaret Formation is a steeply, westward dipping succession of semipelites, feldspar-rich gneisses, psammites and foliated amphibolites. The Vassfaret Formation overlies the Bangenhuken Complex, which comprises well-lineated, medium- to coarse-grained granitic gneisses with subordinate intercalations of metasediments. In the northern part of Ny-Friesland, several E-W striking faults have been identified and most likely joint sets of similar orientation occur (Fig. 1; Dallmann, 2015). The strike of the regional faults shows overall correlation with the orientation of the axis of the tributary fjords and outlet glaciers entering Wijdefjorden.

The topography of the area is undulating and hosts numerous lakes, with Femmilsjøen (surface area: 7.57 km^2) being the largest (Allaart et al., 2021). The postglacial marine limit is mapped at ~65 m a.s.l. in Mosselbukta ~10 km to the north of the mapped region (Fig. 2; Salvigsen and Österholm, 1982). The marine isolation threshold of Femmilsjøen is 26 m a.s.l. and it became isolated from the marine environment between *c.* 11.7 ± 0.3 and *c.* 11.3 ± 0.2 cal. ka BP (Allaart et al., 2021). The overall morphology is described as coastal lowland and further inland towards the front of Midtsundstadbreen as open hilly landscape (Dallmann, 2015).

2.2. Climate and glaciers

Svalbard has a high Arctic climate, characterised by continuous permafrost that underlies at least 90% of the land surface and with a modelled thickness ranging from 100 to 500 m (Humlum et al., 2003; Etzelmüller and Hagen, 2005; Christiansen et al., 2013; Gilbert et al., 2018). The active layer thickness is generally around 1–2 m (Humlum et al., 2003; Hanssen-Bauer et al., 2019; Strand et al., 2020). Mean monthly air temperatures at or above zero occur from June through September during the last decade (MET Norway, 2020; Fig. 3).

The climate of the archipelago is largely controlled by interaction of heat advection in the West Spitsbergen Current (WSC) and the sea-ice covered Arctic Ocean to the north and their associated warm and cold air masses (Aagaard et al., 1987; Hanssen-Bauer et al., 2019; Fig. 1). Arctic amplification prevails, and even small changes in the configuration of the surrounding water and air masses affect the climate of the archipelago. Currently, the climate is getting warmer and wetter, driving glacial retreat and exposing new landscapes that are more prone to erosion (Førland et al., 2011; Berthling et al., 2020). Climate change further affects the geomorphic processes acting in Svalbard. For example, a thickening of the active layer is suggested to enhance slope instability, as well as coastal erosion (Kasprzak et al., 2017; Hanssen-Bauer et al., 2019).

The study area in the northern part of Wijdefjorden is sparsely vegetated and belongs to the northern Arctic Tundra zone (Norwegian Polar Institute, 2019). In Wijdefjorden, the sea-ice minimum (average data from 1980 to 2016) occurs during July through November, when the sea-ice extent is below 20% (Dahlke et al., 2020).

3. Methods

The geomorphological mapping is based on the analysis of aerial images and a 5 × 5 m digital elevation model (DEM) provided by the Norwegian Polar Institute (2010, 2014), as well as field mapping carried out during a field campaign in 2018. Oblique aerial images of the area from 1936, provided by the Norwegian Polar Institute, were used for landscape comparison (Fig. 2). During fieldwork, the area was mapped with a handheld GPS and landforms were described and photographed. The map was created in ESRI ArcMap 10.5 with a zoom level of 1:1500 and finalised in Adobe Illustrator CS6. The map follows the standard for Quaternary geological maps from the Geological Survey of Norway (e.g., Rubensdotter et al., 2015a, 2015b; Larsen et al., 2018), with some additional features unique to the mapped area. The map covers an area of 62 km^2. Bathymetric data of Femmilsjøen and Austre Nevlingen are modified from Allaart et al. (2021) and Kjellman et al. (2020).

4. Geomorphology and surficial geology map units

The low-relief coastal lowlands are characterised by sets of terraces with coastal landforms and marine sediments. The marine sediments are traceable along the shores of Femmilsjøen and thus occur up to ~8 km inland. The uppermost marine deposits occur at ~72 m a.s.l., which

Fig. 4. (a) Overview map of the Femmilsjøen area, locations of elevation profiles are marked with black lines. (b) W-E elevation profile. (c) S-N elevation profile of the low-relief terrain dominated by raised glaciomarine deposits and beaches, parallel to Wijdefjorden. (d) S-N elevation profile of the plateau area in proximity to the ice margin. The terrain is cut by Femmilsjøen where the elevation decreases significantly. DEM © Norwegian Polar Institute.

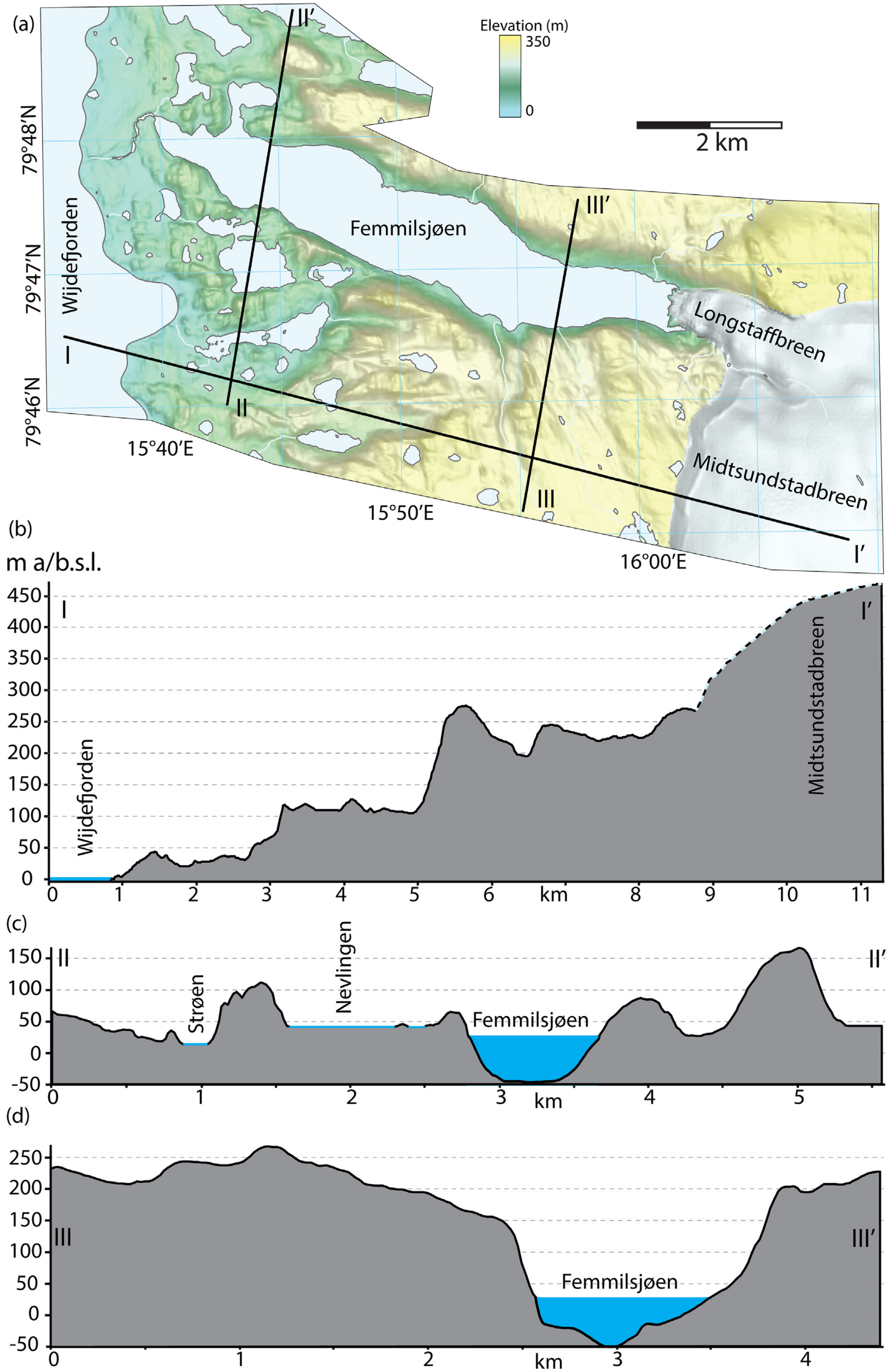
(a)
Elevation (m)
350
0
2 km
III'
III'
Femmilsjøen
Wijdefjorden
79°48'N
79°47'N
79°46'N
Longstaffbreen
Midtsundstadbreen
I
II
III
I'
15°40'E
15°50'E
16°00'E
(b)
m a/b.s.l.
450
400
350
300
250
200
150
100
50
0
I
I'
Wijdefjorden
Midtsundstadbreen
0
1
2
3
4
5
6
km
8
9
10
11
(c)
150
100
50
0
-50
II
II'
Strøen
Nevlingen
Femmilsjøen
0
1
2
3
km
4
5
(d)
250
200
150
100
50
0
-50
III
III'
Femmilsjøen
0
1
2
km
3
4

is ~7 m higher than previously mapped in Mosselbukta, ~10 km to the north of the study site (Fig. 1a; Salvigsen and Österholm, 1982).

The transition from coastal lowland to the mountain plateau is characterised by steep terrain with small lakes in depressions and slope deposits dominating the landscape (Fig. 4a). Brennkollen (282 m a.s.l.) is the most prominent peak in the mapped area.

The mountain plateau is low-relief terrain extending from about 5 km inland and up to (and likely beyond) the glacier margin (yellow area on Fig. 4a). The elevation of the plateau ranges from ~220 m a.s.l. to ~287 m a.s.l. The plateau is dominated by rolling, in situ weathered bedrock hills and periglacially altered surfaces in between. Perennial snow patches are abundant. The glacier front is steep, and ~50 m up-glacier, there is a supraglacial ridge with diamictic composition running parallel to the ice margin. In the following section, the mapped landforms and surficial sediments (Table 1; Fig. 5) are presented in chronological order of formation.

4.1. Landforms from the last glaciation

4.1.1. Exposed bedrock

Exposed bedrock is abundant across the entire mapped area. Fractures are observed in the bedrock surface immediately in front of the ice margin (Fig. 9a). Striated bedrock (~270°) occurs south of Strøen and west of Nevlingen, below the marine limit in the coastal area (Figs. 2 and 5). The striated bedrock is interpreted to have experienced scouring by erosive ice, streaming in an E-W direction (Kleman, 1990; Benn and Evans, 2010). The fractures in the bedrock in front of the ice margin are interpreted as small-scale indicators of subglacial erosion (Cuffey et al., 2000). Exposed bedrock constitutes 7.25 km^2 of the mapped area.

4.1.2. Periglacially altered till surface

A thin silt-rich, fine grained diamict deposit with a periglacially altered surface (sorted circles, diameter up to 4 m, and stripes; Humlum et al., 2003; French, 2018) occurs on the bedrock plateau in the eastern part of the study area (Figs. 5 and 10). The exact thickness is undefined, and the deposit is in some areas cut by drainage channels. Smaller patches also occur in the low-lying coastal terrain, below the marine limit (Fig. 6). Etzelmüller and Sollid (1991) suggested that the presence of silt-rich, fine-grained material is a precondition for sorted circles to form, and we interpret the sediment on the bedrock plateau to represent a thin till cover deposited during full glacial conditions. The thin till cover has provided the fine sediments to allow the sorted circles to form. In total, it constitutes 3.06 km^2 of the mapped area.

Table 1
Mapped landforms and surficial deposits, area (km^2), and area coverage (%).

Landform or sediment type	Area (km^2)	Area coverage (%)
Beach deposit, modern	0.13	0.21
Beach deposit, raised	1.94	3.14
Blockfield	7.17	11.59
Colluvial fan	1.32	2.13
Exposed bedrock	7.25	11.72
Fluvial and glaciofluvial deposit	2.50	4.04
Glacier	11.90	19.24
Kame terrace	0.01	0.02
Lacustrine deposit	0.68	1.20
Lakes and rivers	11.93	19.29
Marginal moraine	0.02	0.03
Periglacially altered till surface	3.06	4.95
Raised fine-grained glaciomarine deposits	3.58	5.78
Rock glacier	0.06	0.10
Supraglacial thrust ridge	0.43	0.70
Solifluction material	3.37	5.45
Snow patch	2.49	4.03
Talus covered slopes	4.01	6.48

4.2. Landforms from the last deglaciation

4.2.1. Boulders

Large boulders (up to 3 m) are widespread across the mapped region (Figs. 5–11). Some boulders of local lithology appear immediately below slopes and are rock-fall deposits. However, most of the boulders are of exotic lithologies and interpreted as erratics deposited during glacial retreat. The boulder symbol on the map indicates presence of boulders in a certain area.

4.2.2. Marginal moraines

One clearly defined ridge (1 m high, 3 m wide, and 45 m long) with angular to sub-rounded boulders on the surface and an interior of diamict with sub-rounded clasts and shell fragments occur in the NW part of the study area south of Gunvorvatnet. The orientation of the ridge is parallel to the coast and the ridge is interpreted as a marginal moraine. Another distinct ridge, also interpreted as a marginal moraine, occurs in the SE part of the study area immediately in front of the glacier margin of Midtsundstadbreen (Figs. 5 and 10). Three less distinct ridges interpreted as remnants of lateral moraines occur on a slope SE of Brennkollen (Figs. 5 and 8) and one has been identified on the northern slope in the western end of Femmilsjøen (Fig. 5).

4.2.3. Features marking former ice-margin positions

On the bedrock ridge above the western shore of Femmilsjøen, a distinct border separates raised beach deposits to the east and bedrock to the west (Fig. 6). Inactive fluvial channels descend towards west, away from the border, and the abundance of large erratics (>1 m) is high. We interpret this border as a former ice-margin position, and that the beach deposits on the eastern part of the ridge have formed subsequent to ice retreat. Four additional ice-marginal positions have been identified in the coastal lowland. Their general appearance is subtle, however all positions are characterised by higher concentrations of erratics. One ice-marginal position in the western end of Helgevatnet is identified by the presence of a terrace-shaped deposit consisting of sand and gravel, interpreted as a kame terrace, deposited in an ice-dammed lake (e.g., Donelly and Harris, 1989; Fig. 5).

4.3. Raised marine deposits

4.3.1. Raised fine-grained glaciomarine deposits

Fine-grained, compact diamict sediments with sporadic clasts dominate the coastal area and the lower shores of Femmilsjøen, generally below 72 m a.s.l. (marine limit in Mosselbukta 10 km north ~65 m a.s.l.; Figs. 5–7). The diamict sediments drape the underlying terrain and covers 3.58 km^2 of the mapped area. Bivalve mollusc shell fragments (mainly of *Mya truncata* and *Hiatella arctica*) are abundant. We interpret the deposit to represent raised marine sediments deposited in a glaciomarine environment, prior to postglacial glacioisostatic rebound, similar to previous observations in the region (Salvigsen and Österholm, 1982; Brückner and Schellman, 2003; Dallmann, 2015). The composition of the raised marine deposits is similar to observations of glaciomarine sediments in lake and marine sediment cores from the Femmilsjøen area (Allaart et al., 2020, 2021).

4.3.2. Raised beach deposits

Up to 500 m wide deposits of sand and gravel occur at elevations from ~3 to ~72 m a.s.l., predominantly along the modern coastline of Wijdefjorden and up to 3.3 km inland (Figs. 5–7). Grain sizes vary from coarse sand up to small boulders. Distinct ridges (~0.2 m high) occur. The deposits are interpreted as raised beach deposits and constitute 1.94 km^2 of the mapped area (Salvigsen, 1978). Compared to the modern beaches, the deposits are dominated by coarser material and shell fragments are rare. The uppermost occurrence of raised beach deposits represents the postglacial marine limit in the area and corresponds relatively well to the marine limit of 65 m a.s.l. towards the

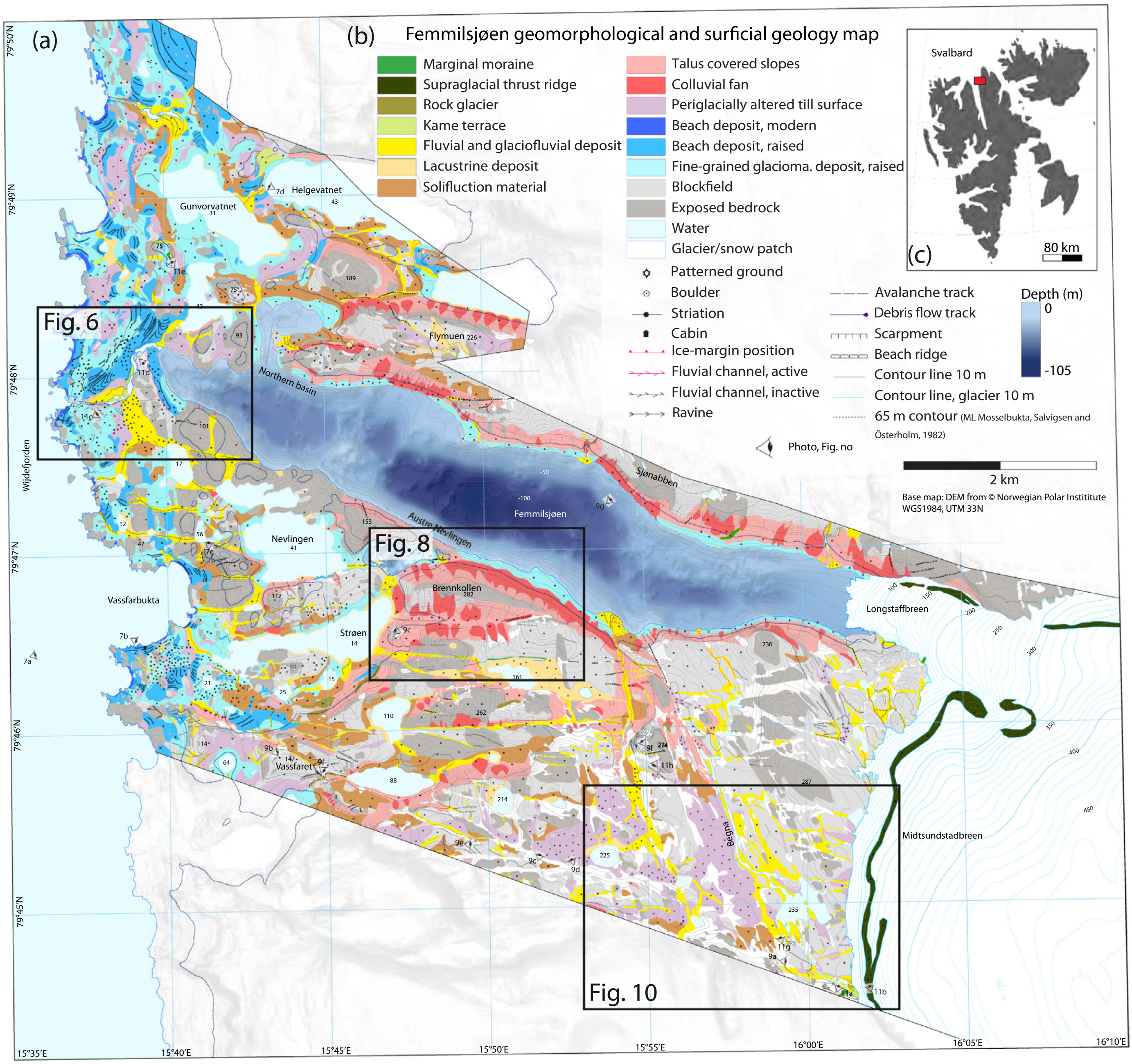

Fig. 5. (a) Geomorphological and surficial geologic map of the area surrounding Femmilsjøen, from Wijdefjorden in the west to Midtsundstadbreen in southeast. Locations of Figs. 6, 8 and 10 are marked with black boxes. (b) Legend. (c) Inset map of Svalbard, study area is marked with a red box. A full resolution version of Fig. 5 is available as online Supplementary Fig. S1.

mouth of the fjord in Mosselbukta (Fig. 1a; Salvigsen and Österholm, 1982).

4.4. Landforms of fluvial origin

4.4.1. Fluvial and glaciofluvial deposits

In the low-relief terrain parallel to the coast, channels with longitudinal bars of sorted sand and gravel as well as boulders occur (Figs. 5 and 6). The channels are oriented primarily perpendicular to and gently sloping towards the coast (Figs. 5 and 6). In a few of the channels, streams of running water occur and are mapped as *fluvial channel, active*. Similar channels occur on the plateau in front of Midtsundstadbreen, however there the orientation and gradient are predominantly towards north, parallel to the ice-margin and the channels drain into Femmilsjøen, where small deltas form (Figs. 5 and 10). Most of the active streams occur in the channels close to the glacier front. On the surface of the glaciofluvial deposits, periglacial landforms such as sorted circles and stripes occur. Fluvial and glaciofluvial deposits cover 2.50 km^2 of the mapped area.

4.4.2. Incised channels

Channels up to 12 m deep and 50 m wide incised in bedrock occur at the outlets of Gunvorvatnet, Femmilsjøen, and the unnamed lake SE of Vassfaret, as well as along the paths of the fluvial channels entering Femmilsjøen (Fig. 5). Based on the presence of resistant bedrock in the area, as well as the size of the incisions, we assume that the incisions are old and progressive with phases of erosion during deglaciations. They could have formed as subglacial gorges,

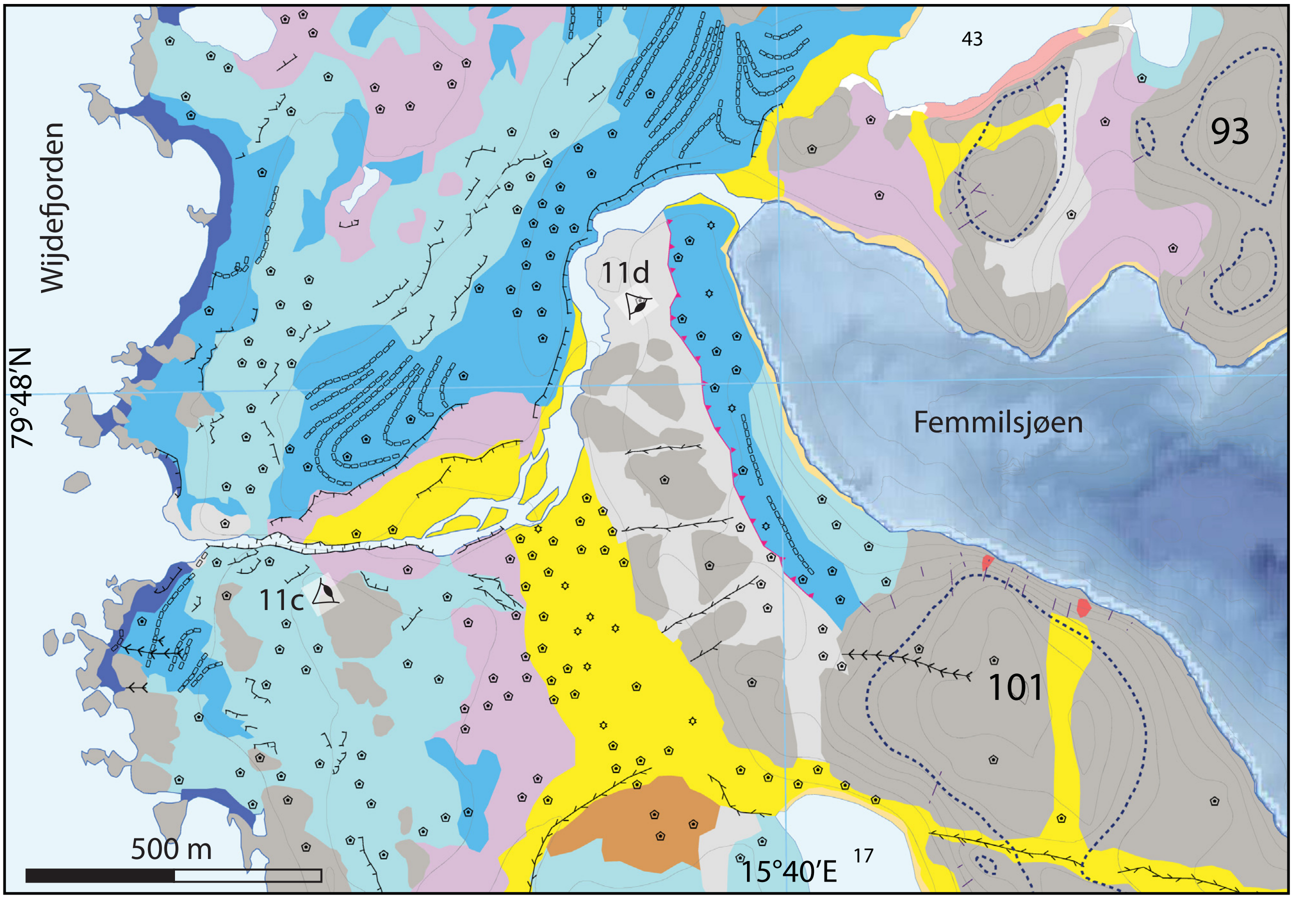

Fig. 6. Detail map of the area around the outlet of Femmilsjøen. The landscape is characterised by raised beaches and marine sediments and deposits, fluvial channels and outcropping bedrock. The area is scattered by boulders/erratics and sorted circles appear on the periglacially altered till surface. For legend, see Fig. 5b.

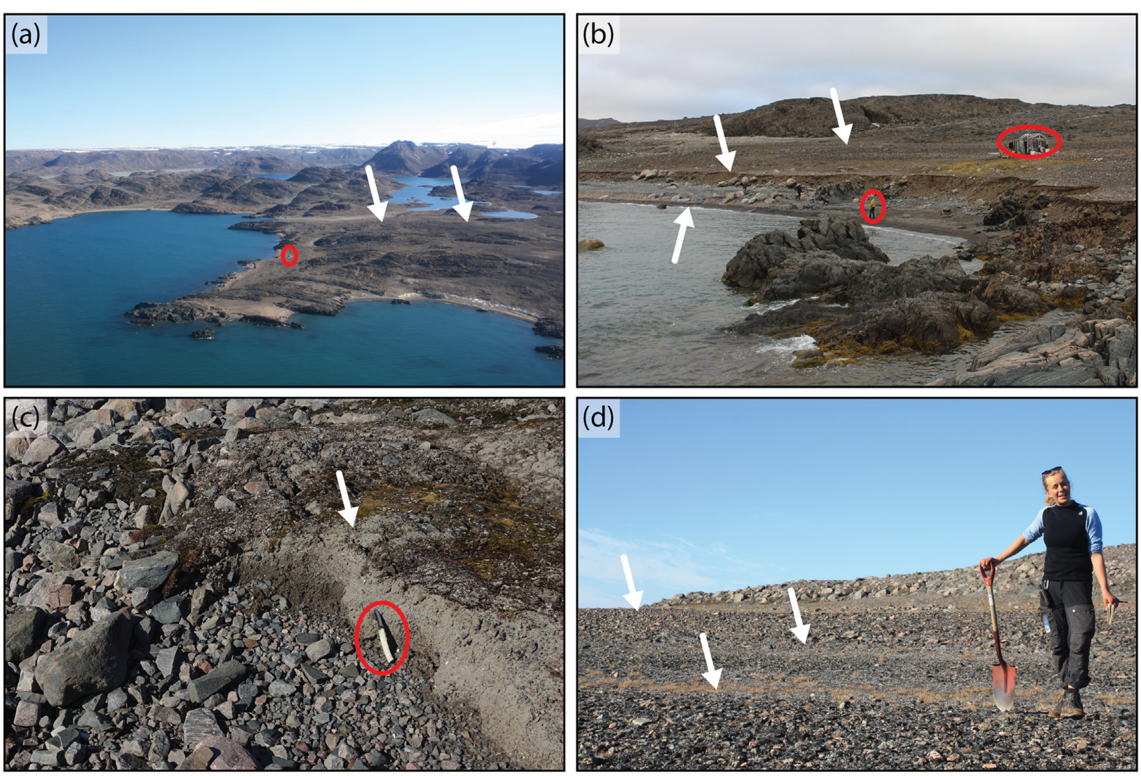

Fig. 7. (a) Oblique image of the coastline SW of Femmilsjøen. The coastline is irregular with several small bays and beaches in between outcropping bedrock. White arrows indicate location of a potential ice-marginal position. Cabin, circled in red, for scale. (b) Modern and raised shorelines (indicated by white arrows), around the cabin (circled in red). Two raised beach ridges are mapped. (c) Raised, glaciomarine diamict with abundant shell fragments. Knife for scale. (d) Beach ridge system between Gunvorvatnet and Helgevatnet. For locations, see Fig. 5.

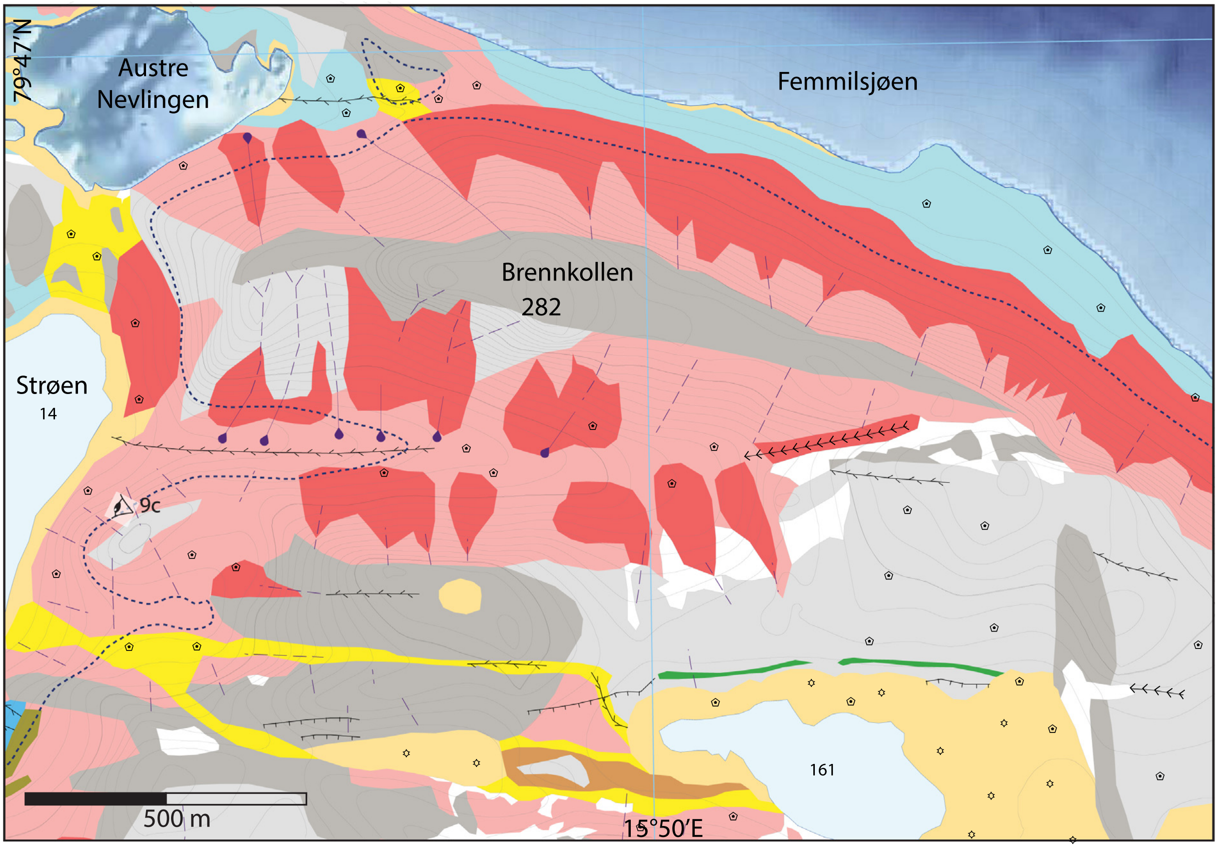

Fig. 8. Detailed map of Brennkollen (282 m a.s.l.), southern shore of Femmilsjøen, showing characteristic slope processes that occur on the steeper terrain in the Femmilsjøen area. The slopes of Brennkollen are covered with a thin layer of talus and at the foot of the hill, colluvial fans of avalanche and debris flow deposits accumulate. Large boulders occur across the entire area. At the summit of Brennkollen, weathered bedrock is exposed. Lacustrine sediments occur in the depressions. For legend, see Fig. 5b.

or by short-lived fluvial erosion during ice retreat, comparable to studies from Iceland (Baynes et al., 2015). However, where channels are incised into sediments, they are more likely to be of Holocene age.

4.5. Landforms of Holocene origin

4.5.1. Blockfields

Fields of large angular boulders of local lithologies mostly or completely covering the surface constitute 7.17 km^2 of the mapped area. The angularity indicates frost weathering and the areas have been mapped as blockfields (Figs. 5, 6 and 9–11; Thompson, 1953; French, 2018). They dominate the plateaus across the entire mapped area. These regions of blockfields have likely been active through the Holocene, however may have been revitalised or relict from previous ice-free periods.

4.5.2. Talus covered slopes, colluvial fans and rock glaciers

The steep slopes are covered by angular, scattered talus (4.01 km^2 of the mapped area) interpreted to originate from weathering processes and rock falls. The steep slopes surrounding Femmilsjøen, as well as the slopes of the highest summits in the area, are dominated by fans of angular debris, interpreted as colluvial fans composed of avalanche and debris-flow deposits (de Haas et al., 2015; Rubensdotter et al., 2015a, 2015b; Farnsworth et al., 2017; Larsen et al., 2018; Figs. 5 and 9). Undulating ridges with coarse debris on the surface occur at the foot of a few NW facing slopes, south of Femmilsjøen (Fig. 5). The ridges are interpreted to be pressure ridges caused by the flow of ice-cemented talus at the toe of the colluvial fans. These features are interpreted as rock glaciers (0.06 km^2; Humlum et al., 2007; Eckerstorfer et al., 2013).

4.5.3. Solifluction material

The gentler slopes are dominated by a thin soil cover, where creep occurs in the active layer, and the area is mapped as solifluction material (e.g., Harris et al., 2011; Rubensdotter et al., 2015a, 2015b; Larsen et al., 2018). Solifluction material makes up 3.37 km^2 of the mapped area (Figs. 8 and 9).

4.5.4. Lacustrine deposits

Fine-grained deposits (primarily silt) occur along the lake shores and in depressions across the entire area (Fig. 8). Some of the lake shorelines are dominated by coarser gravel. The deposits occur up to ~1 m above the current lake surfaces. Both the fine- and coarse-grained materials are interpreted to be remnants after higher lake levels, and the coarseness to reflect variable degrees of erosion and transport. Higher lake levels could be explained by a former higher base level during periods of higher sea level or higher meltwater supply to the lakes due to more glacier proximal conditions. Alternatively, it could be explained by increased precipitation in the area during the Holocene Thermal Maximum (HTM) similar to observations from the western Arctic (Barber and Finney, 2000; Kaufman et al., 2004) and in agreement with regional precipitation reconstructions (Kjellman et al., 2020). Expansion of taliks below shallow lakes without distinct outflows could also lower the lake levels (e.g., Burn and Smith, 1990).

4.5.5. Modern beach deposits

Deposits of sand and gravel (up to 70 m wide) with actively forming ridges (~0.3 m high), separated by outcropping bedrock of positive relief, occur in the bays along the coast of Wijdefjorden (Figs. 2, 5–7). The deposits are found up to 3 m a.s.l. and constitute 0.13 km^2 of the

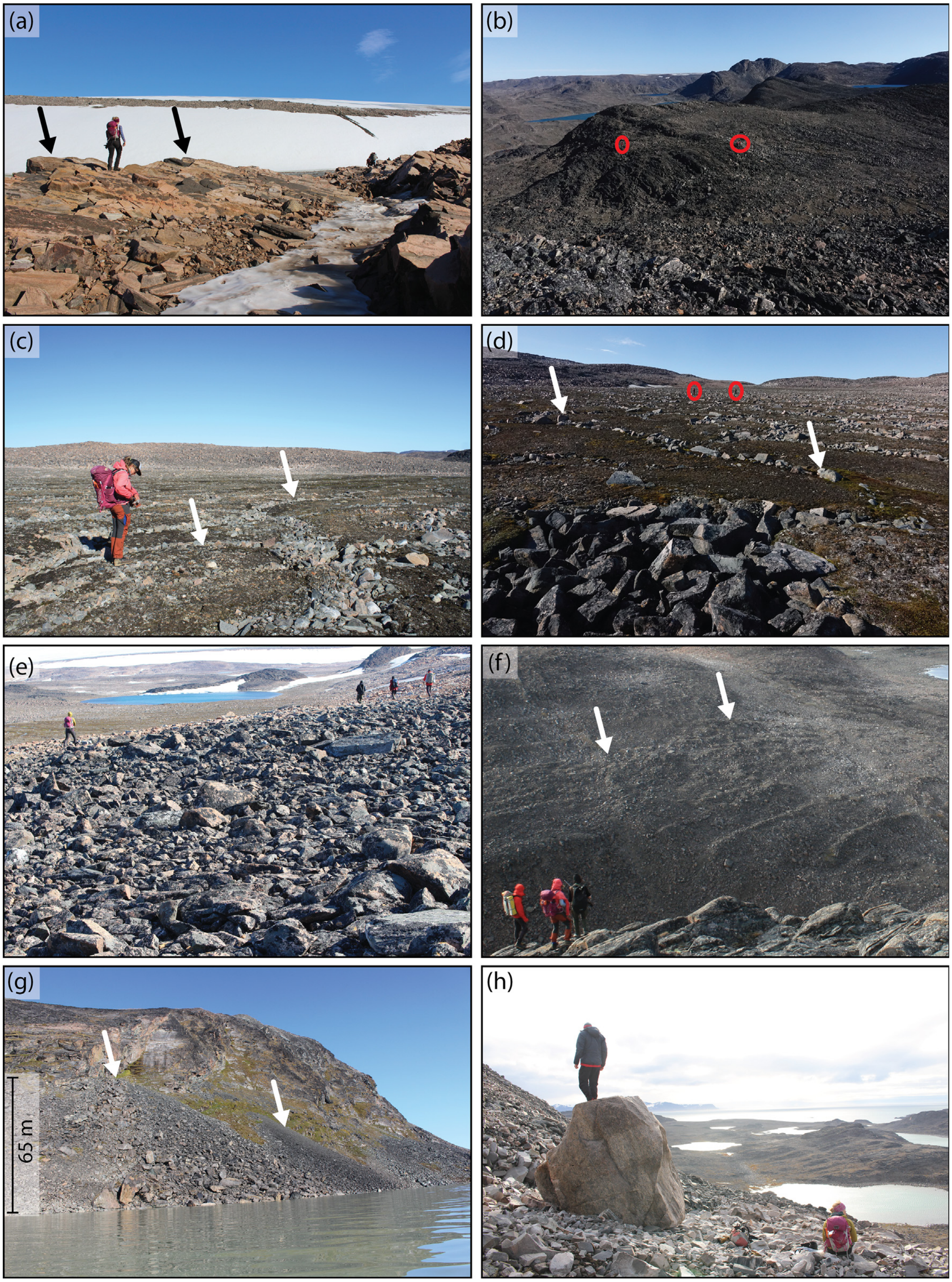

Fig. 9. (a) Black arrows point to exposed, weathered bedrock at the present day ice-margin of Midtsundstadbreen. (b) Blockfield, persons circled in red for scale. (c) Periglacially altered till surface with sorted circles. (d) Periglacially altered till surface with sorted stripes. (e) Blockfield. (f) Solifluction lobes. (g) Colluvial fans (avalanche and debris flow deposits) on the northern shore of Femmilsjøen. (h) Large boulder on slope with talus. For locations, see Fig. 5.

mapped area (Table 1). On the modern beaches, driftwood is abundant, but only very few mollusc shells occur. The deposits are interpreted as modern fair-weather beach ridges similar to observations across Wijdefjorden, in Mosselbukta, and elsewhere in Svalbard (Thompson, 1953; Salvigsen, 1978; Salvigsen and Österholm, 1982; Brückner and Schellman, 2003; Sessford et al., 2015).

4.5.6. Supraglacial thrust ridge

Approximately 50 m inboard of the margin of Midtsundstadbreen, there is an 85 m wide debris band running parallel to the ice front (Figs. 5 and 10). It has a diamictic composition and large boulders are abundant on the surface. The landform is strikingly similar to thrust moraines observed in northern Greenland, where the material is

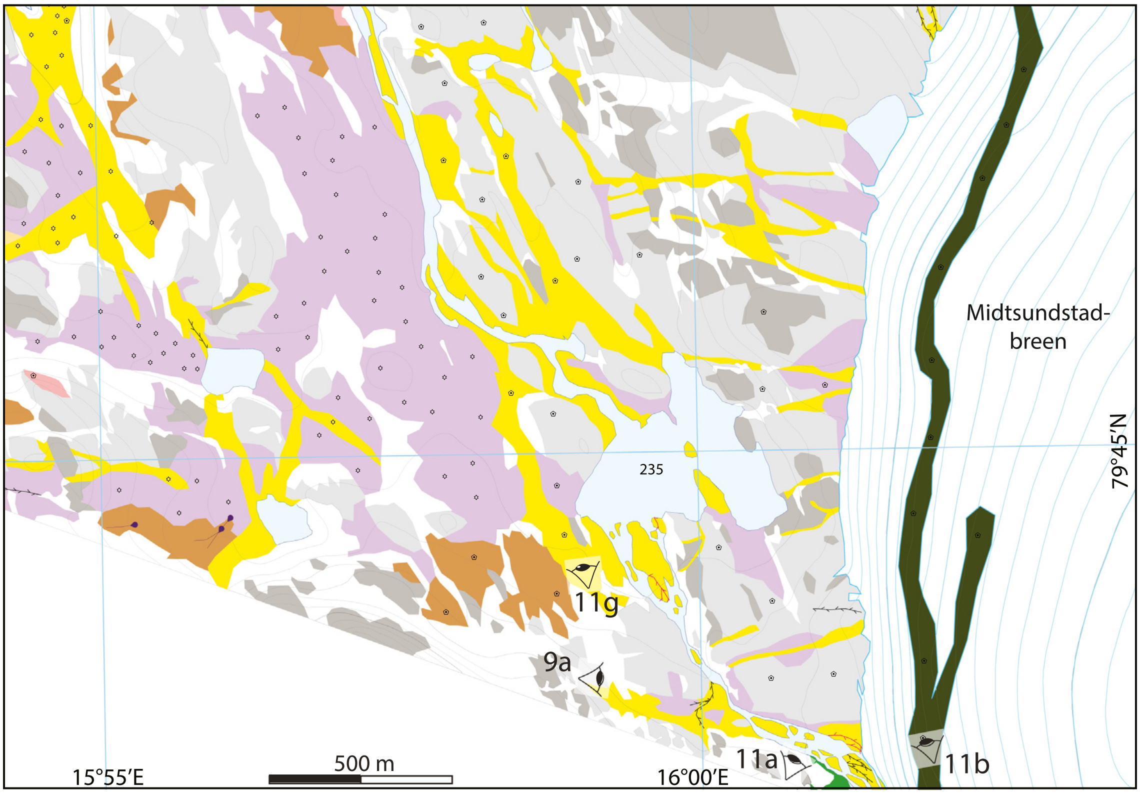

Fig. 10. Detailed map of the glacier front of Longstaffbreen. For legend see Fig. 5b.

interpreted to be brought up to the surface along thrust planes in the ice (Bishop, 1957; Boulton, 1967). Hambrey et al. (1997) suggest that thrusting is particularly common in the transition zone from warm interior ice to a frozen snout, where the ice undergoes strong longitudinal compression. We interpret the supraglacial moraine as a thrust moraine that has formed and possibly still is forming at such a transition zone.

5. Discussion

5.1. Temporal and spatial significance of landform and surficial deposit distribution

The faint traces of striae on the bedrock in the coastal lowland, the thin till cover on the bedrock plateau, as well as the scattered erratics of exotic lithologies are landforms that belong to the last glaciation, when the Femmilsjøen area was covered by grounded ice (Allaart et al., 2020, 2021). The incised channels are most likely older and progressive with phases of erosion. The composition of the raised glaciomarine deposits is comparable to findings from marine and lake sediment cores from Wijdefjorden and Femmilsjøen, from where it has been suggested that Femmilsjøen was connected to the fjord until between 11.7 and 11.3 cal. ka BP (Allaart et al., 2020, 2021). The raised beach ridges are the results of gradual emergence after the deglaciation (Forman et al., 2004). The marine deposits and beach ridges above the isolation threshold of Femmilsjøen (26 m a.s.l.) must thus have been deposited prior to the isolation (Fig. 11). Periglacial processes initiated concurrently with or shortly after deglaciation of the area (Humlum, 2005; Fig. 12). Slope processes would have initiated on the steep slopes shortly after deglaciation, comparable to studies of rockwall retreat in Svalbard (Berthling and Etzelmüller, 2007; Siewert et al., 2012; Eckerstorfer et al., 2013; Berthling et al., 2020).

There are very few ice-marginal deposits in the mapped area. However, we suggest that the ice marginal positions mapped in the low-relief coastal area represent dynamic re-advances of tributary glaciers after retreat of the main glacier in Wijdefjorden, similar to observations on Andrée Land (across Wijdefjorden), and elsewhere in Svalbard (Fig. 1; Brückner and Schellman, 2003; Lønne, 2005; Farnsworth et al., 2017, 2018b, Larsen et al., 2018; Farnsworth et al., 2020b). Due to the wave-washed appearance of the mapped ice margin positions, we interpret that the re-advances occurred into a high relative sea level prior to extensive glacioisostatic uplift (Figs. 5 and 11). However, no distinct sediment layer indicative of re-advance is observed in lake sediment cores from Femmilsjøen and better chronological control is needed in order to assess the timing of re-advances (Allaart et al., 2021).

Previous studies in the area have implied that the HTM was warm and wet, and that glaciers had retreated out of the catchment area of Femmilsjøen at this time (Allaart et al., 2020, 2021; Kjellman et al., 2020). During the HTM, permafrost was likely less extensive in the Femmilsjøen area, the active layer was thicker and periglacial processes more widespread as glaciers covered less of the Svalbard landscape). Periglacial processes, like today, were controlled by the frequency and rate of freeze and thaw as well as the moisture conditions of the substrate. Permafrost is suggested to have re-established in the lowlands of Svalbard *c.* 3.0 cal. ka BP, and this is likely possible for the Femmilsjøen area as well (Gilbert et al., 2018). The abundant sorted circles and their clear sorting indicate that frost-heave processes are active today.

5.2. Emergence and the highest coastline

The occurrence of marine deposits up to 72 m a.s.l. aligns well with a progressive in-fjord higher marine limit. Thus the Femmilsjøen marine limit is at slightly higher elevation than the marine limit on the sea-level curve from Mosselbukta (Figs. 5 and 6; Salvigsen and Österholm, 1982). The difference of ~7 m indicates that the uplift has been more extensive around Femmilsjøen compared to Mosselbukta, and also that the ice thickness and duration of ice cover was greater 10 km farther south during the Late Weichselian. A lower marine limit on the

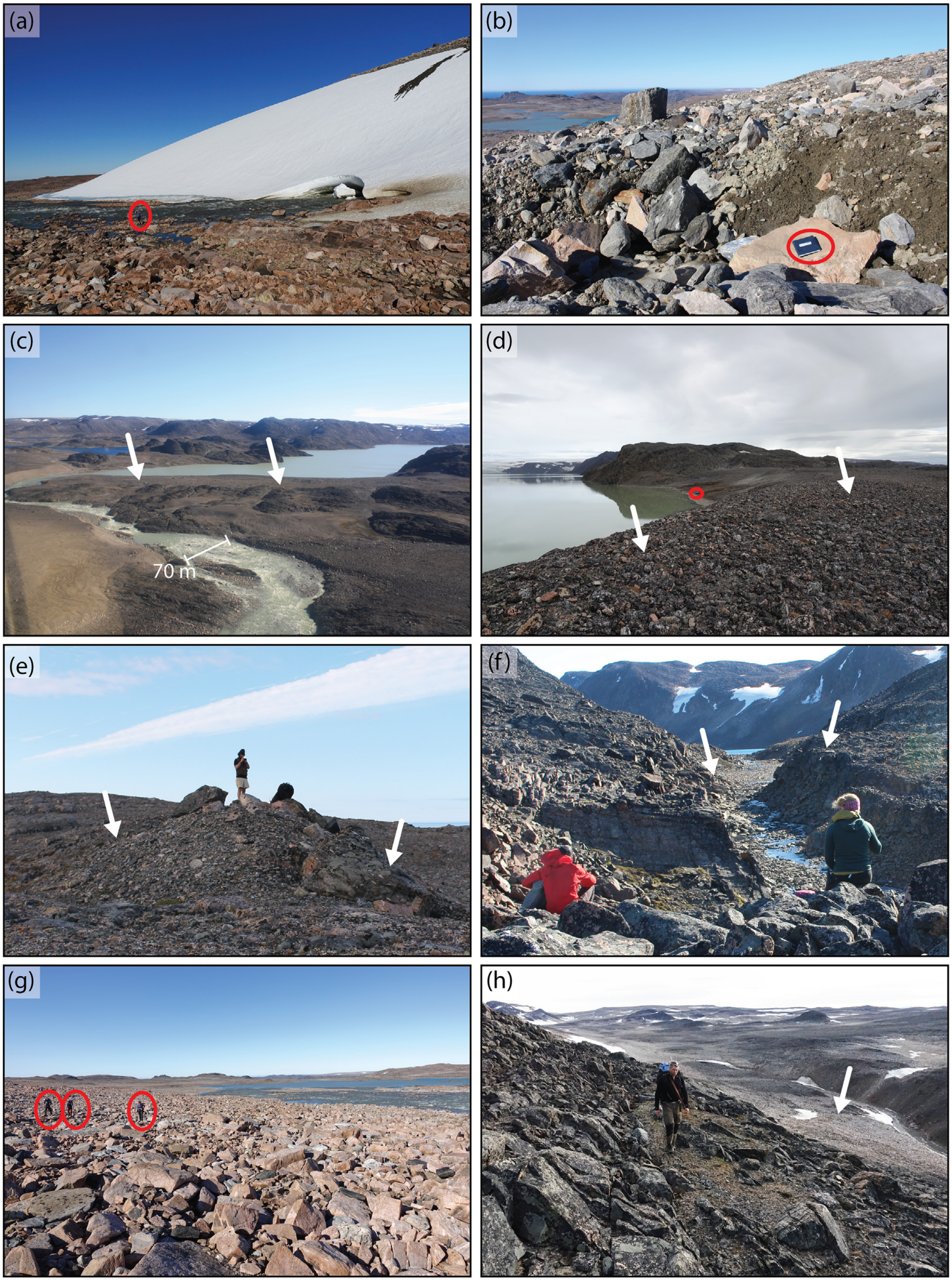

Fig. 11. (a) Ice margin of Midtsundstadbreen, person circled in red for scale. The moraine is visible in the upper right corner. (b) Moraine on Midtsundstadbreen. Notebook for scale. (c) Outlet of Femmilsjøen, white arrows indicate possible ice-marginal position. (d) Ridge above the outlet of Femmilsjøen, possible ice-marginal position which subsequently has been washed out by waves due to high relative sea level. The surface morphology is beach. (e) Possible ice-marginal position, ridge with shell fragments. (f) Incised channel in bedrock. (g) Outwash plane in front of Midtsundstadbreen, people circled in red for scale. (h) Inactive fluvial channel.

peninsula in the outer-fjord is not unusual given that the postglacial marine limit is governed by a combination of ice cover thickness, duration and the timing of deglaciation (Blake, 1962; Forman et al., 2004; Farnsworth et al., 2020a).

5.3. Character of deglaciation and ice dynamics of Midtsundstadbreen

The thermal state of Svalbard glaciers has been documented to switch from polythermal to cold-based during retreat and thinning, as thinning

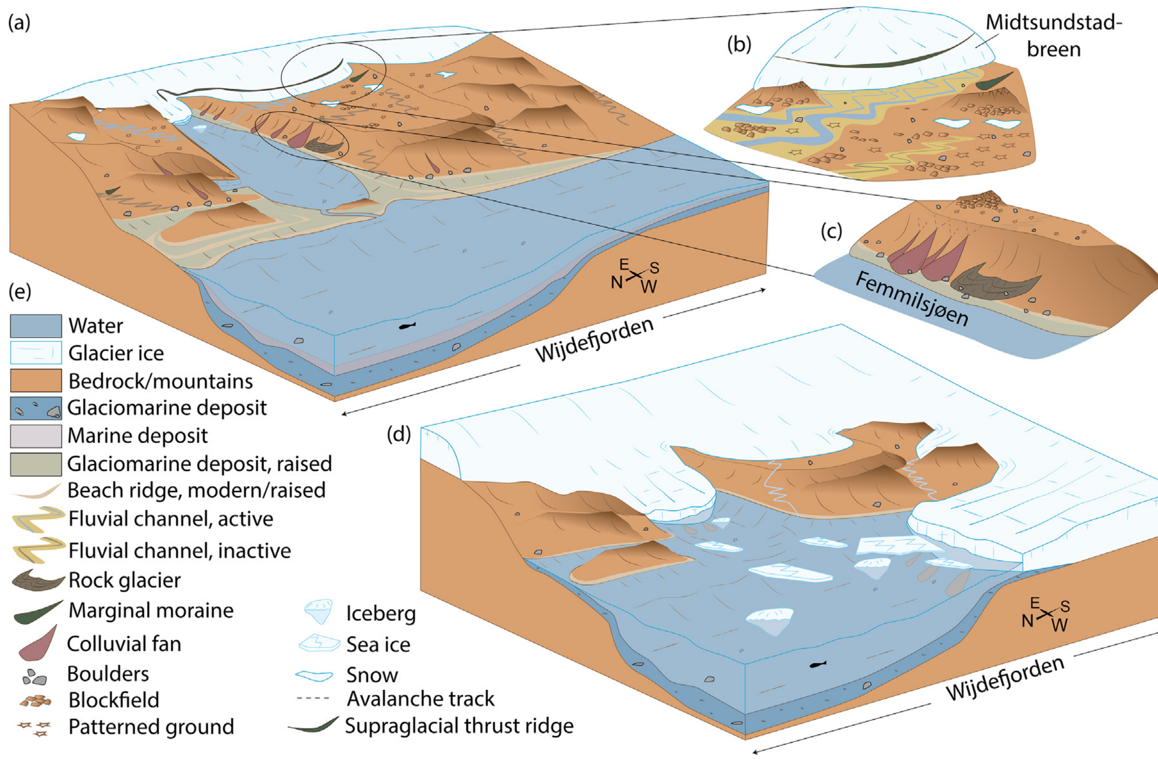

Fig. 12. Conceptual model of the depositional environments in the Femmilsjøen area. (a) Model of the present morphology. (b) Details of the ice front of Midtsundstadbreen: glaciofluvial processes, ice-marginal processes, weathering, periglacial landforms. (c) Weathering and slope processes taking place around Femmilsjøen. (d) Early deglaciation of the Femmilsjøen area, high relative sea level and glaciomarine deposition in the submerged areas. (e) Legend.

allows for penetration of cold atmospheric temperatures to the bed of the ice (e.g., Hagen et al., 1993; Lovell et al., 2015; Farnsworth et al., 2020b). Midtsundstadbreen could have switched from warm to cold after the LGM, and as the ice sheet in the northern sector had already started thinning *c.* 25 ka ago, the switch may have occurred early (Gjermundsen et al., 2013). However, while most of the case studies of thermal switch are from small valley glaciers, we assume that it would also occur within large ice caps (e.g., Humlum et al., 2005; Lovell et al., 2015).

Cold-based glaciers were for a long time thought to protect the substrate rather than modify it (Glasser et al., 2020, and references therein). During the last two decades, this view has been challenged by studies indicating that cold-based glaciers modify landscapes, however, at a rate of an order of magnitude lower (Cuffey et al., 2000; Atkins et al., 2002; Atkins, 2013). Studies from Antarctica have identified geomorphological evidence of cold-based glacier activity (Atkins et al., 2002, Atkins, 2013). Examples of identified erosional features are broad scrapes and grooves, irregular scuffs, scrapes and scratches of exposed boulders embedded in pre-existing glacial deposits and meltwater channels, and examples of depositional features include thin patchy drift, boulder belts or drop moraines, boulder trains and scattered boulders, resembling our observations from the Femmilsjøen area (blockfields, meltwater channels parallel to the ice-margin, scattered boulders, etc., Figs. 4–11; Atkins, 2013). The periglacially altered till surface on the bedrock plateau closely resembles thin till deposits from cold-based glaciers in Antarctica (Atkins, 2013). Furthermore, Martín-Moreno et al. (2017) mapped the Little Ice Age (LIA) extent across Svalbard based on the online available map resources from the Norwegian Polar Institute. Significantly, no traces of LIA advances were mapped around the NW margin of Åsgardfonna (including Longstaffbreen and Midtsundstadbreen), and they attributed the lack of LIA moraines and ice marginal deposits to cold-based glacier fronts. The few striations mapped in the Femmilsjøen area occur in the low-relief coastal area, and none were observed on the bedrock plateau, suggesting that only in the lower elevation areas, the ice was at the pressure melting point at the base and thus able to abrade the bedrock. This scenario is similar to studies from Nordaustlandet, where it has been suggested that the warm-based part of the ice sheet during the Late Weichselian was confined to fjords and lowlands below 200–230 m a.s.l., and that cold-based ice covered the higher elevated terrain (Hormes et al., 2011; Gjermundsen et al., 2013). This is comparable to observations from NW Iceland, where cold-based areas are suggested to have prevailed above ~500 m a.s.l. (Brynjólfsson et al., 2015). Similarly, it is suggested that Reinsdyrflya (~45 km west of Midtsunstadbreen; Fig. 1) was an inter-ice-stream area during the Late Weichselian, with cold-based ice covering the strandflat and limited glacial imprints left in the area (Gjermundsen et al., 2013). The very limited glacial imprints on the bedrock plateau, the comparability to landscapes of cold-based glaciers in Antarctica, the presence of the thrust moraine, as well as the similar overall elevation of the bedrock plateau (>200 m a.s.l.) to the suggested cold-based zones in Nordaustlandet, support the idea that predominantly cold-based ice has covered the bedrock plateau during the Late Weichselian.

An alternative to a cold-based glacier interpretation to the lack of bedrock-erosional features on the plateau is the idea that the lithological and structural properties of the bedrock substratum in itself may influence the erodibility of the covering glacier ice, and thus limit the formation of subglacial erosional landforms (Glasser and Kabbendam, 2011; Kelly et al., 2014). Hard substratum as such in the Femmilsjøen area and the presence of unfavourable structures are known to slow the rate of subglacial erosion. Narrow joint spacing has been suggested to favour quarrying and higher erosion rates, while more widely spaced joints favour abrasion and lower rates of erosion of the landscape (Dühnforth et al., 2010; Glasser and Kabbendam, 2011). The foliation in the study area is dominantly N-S striking and westward dipping (Dallmann, 2015). It has been suggested that tributary glaciers in the region exhibited dynamic advances subsequent to retreat of the main glacier in Wijdefjorden after LGM (Salvigsen and Österholm, 1982; Furrer et al., 1991; Farnsworth et al., 2020b). If these dynamic post-LGM advances were across the plateau towards the west and thus oriented normal to the low-relief bedrock structures, quarrying could have been favoured over abrasion, and could explain the lack of striations on the bedrock plateau (Glasser et al., 1998; Dühnforth et al., 2010; Glasser and Kabbendam, 2011).

However, subglacially deposited landforms that are subaerially exposed are prone to weathering, and as the area had potentially deglaciated already by *c.* 16.0 cal. ka BP, that would leave substantial time for weathering to erode any potentially deposited landforms (Ballantyne, 2002). Based on the field evidence as well as observations from nearby glaciated areas, we attribute the landscape on the plateau to have been little affected because the glacier was cold-based. The bedrock certainly played a role, but further investigations are needed in order to address the possibility of cold-based ice during the Last Glacial. ^{10}Be, ^{26}Al and in situ ^{14}C cosmogenic exposure dating of the bedrock and erratics from the foreland of Midtsundstadbreen could shed light on the erosion history of the landscape, as well as indicate if the area was covered by warm- or cold-based ice during the Last Glacial (e.g., Bierman et al., 2014; Corbett et al., 2015; Farnsworth et al., 2018a).

The lack of landforms indicative of surge activity, related to advances of the surge-type glacier Longstaffbreen could possibly also be attributed to the regional bedrock (e.g., Farnsworth et al., 2016). Such landforms may exist on the lake floor of Femmilsjøen, and could be investigated through multi-beam mapping of the lake floor.

The few and faint moraine ridges on the bedrock plateau suggest that Midtsundstadbreen was cold-based during its most recent advances. Comparing the aerial images of the area from 1936 and 2010, the location of the thrust moraine on Midtsundstadbreen has not changed, indicating no modification by the 1960s surge of Longstaffbreen (Fig. 2; Hagen et al., 1993; Lønne, 2016). The lack of change in frontal position could reflect that the glacier is in steady state. However, since the overall mass balance of glaciers in Svalbard is negative we interpret it to indicate that the snout of Midtsundstandbreen is currently stagnant and frozen to the ground (Bishop, 1957; Kleman, 1994; Benn and Evans, 2010; Stroeven et al., 2021).

6. Summary and conclusions

Numerous glacier forelands in Svalbard have been mapped, and most of the previous studies focus on morphology and stratigraphy resulting from glaciers. The area studied in this paper, was once entirely covered by glacier ice but exhibits only faint glacial landforms. However, through geomorphological mapping, we have identified processes of deposition and erosion characteristic of the Femmilsjøen area. The landscape indicates that predominantly cold-based ice covered the bedrock plateau during the Late Weichselian.

- The geomorphology of the bedrock plateau in front of Midtsundstadbreen suggests that cold-based ice covered the plateau during the Late Weichselian.
- The coastal zone and areas below 72 m a.s.l. are dominated by raised glaciomarine sediments and beach ridges. In this area, warm-based ice streamed during the Late Weichselian.
- Faint traces of ice-front positions in the low-relief coastal zone are suggested to belong to the deglaciation phase.
- In the transition zone from coastal lowland to the bedrock plateau slope deposits dominate the steeper slopes and slope processes have most likely been active since deglaciation.
- Presently, the snout of Midtsundstadbreen is passive and most likely cold-based. The presence of the thrust moraine may indicate the location of a former transition from warm-based to cold-based ice.
- Periglacial landforms occur throughout the area.

A full resolution version of Fig. 5 is available as online Supplementary Fig. S1. Supplementary data to this article can be found online at https://doi.org/10.1016/j.geomorph.2021.107693.

CRediT authorship contribution statement

LA: conceptualisation, investigation, visualisation, writing, project administration, funding acquisition. AS: conceptualisation, writing, supervision. LH: conceptualisation, writing, supervision. WRF: investigation, funding acquisition, writing. SB: investigation, writing. SEK: investigation, writing. AG: investigation, writing.

LA = Lis Allaart, AS = Anders Schomacker, WRF = Wesley R. Farnsworth, SB = Skafti Brynjólfsson, SEK = Sofia E. Kjellman, LH = Lena Håkansson, AG = Andreas Grumstad.

Declaration of competing interest

The authors declare that they have no known competing financial interests or personal relationships that could have appeared to influence the work reported in this paper.

Acknowledgements

Arve Johnsen (Office of the Governor of Svalbard) provided access to the cabin in Vassfarbukta during fieldwork in 2018. The participants at the annual beach-clean-up of Svalbard are thanked for placing a fuel and wood depot at the field site. Dag Furberg Fjeld and Audun Tholfsen (UNIS logistics) are thanked for help during field preparation and safety checks during fieldwork. Drytech is acknowledged for field lunch supply. Michael Retelle is acknowledged for improving the language and provide constructive feedback prior to submission. Mark Johnson, one anonymous reviewer, and Editor Dr. Achim A. Beylich are thanked for constructive comments that improved the manuscript.

Grant no. 17/01132-3 to Lis Allaart from the Svalbard Environmental Protection Fund covered the main part of fieldwork and laboratory analyses. The field costs for the 2018 campaign were partly funded by Arctic Field grant no. 282643 awarded to Lis Allaart by Svalbard Science Forum/Research Council of Norway, and grant no. 16/35 to Wesley Farnsworth from Svalbard Environmental Protection Fund.

References

Aagaard, K., Foldvik, A., Hillman, S., 1987. The West Spitsbergen Current: disposition and water mass transformation. J. Geophys. Res. Oceans 92, 3778–3784.

Åkerman, J.H., 2005. Relations between slope processes and active-layer thickness 1972–2002, Kapp Linné. Svalbard. Norwegian Journal of Geography 59 (2), 116–128.

Åkerman, J.H., Boardman, J., 1987. Periglacial Forms of Svalbard: a Review. Periglacial Processes and Landforms in Britain and Ireland. Cambridge University Press, Cambridge, pp. 9–25.

Allaart, L., Müller, J., Schomacker, A., Rydningen, T.A., Håkansson, L., Kjellman, S.E., Mollenhauer, G., Forwick, M., 2020. Late Quaternary glacier and sea ice history of northern Wijdefjorden, Svalbard. Boreas 49, 417–437. doi:10.1111/bor.12435.

Allaart, L., Friis, N., Ingólfsson, Ó., Håkansson, L., Noormets, R., Farnsworth, W.R., Mertes, J., Schomacker, A., 2018. Drumlins in the Nordenskiöldbreen forefield, Svalbard. GFF 140, 170–188. https://doi.org/10.1080/11035897.2018.1466832.

Allaart, L., Schomacker, A., Larsen, N.K., Nørmark, E., Rydningen, T.A., Farnsworth, W.R., Retelle, M., Brynjólfsson, S., Forwick, M., Kjellman, S.E., 2021. Glacial history of the Åsgardfonna ice Cap, NE Spitsbergen, since last glaciation. Quat. Sci. Rev. 251, 106717 https://doi.org/10.1016/j.quascirev.2020.106717.

Aradóttir, N., Ingólfsson, Ó., Noormets, R., Benediktsson, Í.Ö., Ben-Yehoshua, D., Håkansson, L., Schomacker, A., 2019. Glacial gemorphology of Trygghamna, western Svalbard – integrating terrestrial and submarine archives for a better understanding of past glacial dynamics. Geomorphology 344, 75–89.

Atkins, C.B., 2013. Geomorphological evidence of cold-based glacier activity in South Victoria Land, Antarctica. Antarctic palaeoenvironments and earth-surface processes. Geological Society of London. Special Publications 381, 299–318.

Atkins, C.B., Barret, P.J., Hicock, S.R., 2002. Cold glaciers erode and deposit: evidence from Allan Hills. Antarctica. Geology 30, 659–662.

Ballantyne, C.K., 2002. Paraglacial geomorphology. Quat. Sci. Rev. 21, 1935–2017.

Barber, V.A., Finney, B.P., 2000. Late Quaternary paleoclimatic reconstructions for interior Alaska based on paleolake-level data and hydrological models. J. Paleolimnol. 24, 29–41.

Baynes, E.R.C., Attal, M., Niedermann, S., Kirstein, L.A., Dugmore, A.J., Naylor, M., 2015. Erosion during extreme flood events dominates Holocene canyon evolution in northeast Iceland. Proc. Natl. Acad. Sci. USA 112, 2355–2360. https://doi.org/10.1073/pnas.1415443112.

Benn, D., Evans, D., 2010. Glaciers and Glaciation. Hodder and Arnold Publication, London, pp. 1–802.

Bennett, M.R., Hambrey, M.J., Huddart, D., Glasser, N.F., Crawford, K., 1999. The landform and sediment assemblage produced by a tidewater glacier surge in Kongsfjorden. Svalbard. Quat. Sci. Rev. 18, 1213–1246.

Bennett, M.R., Huddart, D., Glasser, N.F., Hambrey, M.J., 2000. Resedimentation on an ice-cored lateral moraine in the high-Arctic (Kongsvegen, Svalbard). Geomorphology 35, 21–40.

Berthling, I., Etzelmüller, B., 2007. Holocene rockwall retreat and the estimation of rock glacier age, Prins Karls Foreland. Svalbard. Geogr. Ann. 89, 83–93.

Berthling, I., Berti, C., Mancinelli, V., Stendardi, L., Tommaso, P., Miccadei, E., 2020. Analysis of the paraglacial landscape in the Ny-Ålesund area and Blomstrandhalvøya (Kongsfjorden, Svalbard, Norway). J. Maps 16 (2), 818–833.

Bierman, P.R., Corbett, L.B., Graly, J.A., Neumann, T.A., Lini, A., Crosby, B.T., Rood, D.H., 2014. Preservation of a preglacial landscape under the centre of the Greenland Ice Sheet. Science 344, 402–405.

Bishop, B.C., 1957. Shear moraines in the Thule area, northwest Greenland. Snow, Ice and Permafrost Research Establishment. Corps of Engineers, U.S. Army, Wilmette, Illinois Research Report 17.

Biskaborn, B.K., Smith, S.L., Noetzli, J., Matthes, H., Vieira, G., Streletskiy, D.A., Schoeneich, P., Romanovsky, V.E., Lewkowicz, A.G., Abramov, A., Allard, M., Boike, J., Cable, W.L., Christiansen, H.H., Delaloye, R., Diekmann, B., Drozdov, D., Etzelmüller, B., Grosse, G., Mauro, G., Ingeman-Nielsen, T., Isaken, K., Ishikawa, M., Johansson, M., Johansson, H., Joo, A., Kaverin, D., Kholodov, A., Konstantinov, P., Kröger, T., Lambiel, C., Lanckman, J.-P., Luo, D., Malkova, G., Meiklejohn, I., Moskalenko, N., Oliva, M., Phillips, M., Ramos, M., Sannel, A.B.K., Sergeev, D., Seybold, C., Skryabin, P., Vasiliev, A., Wu, Q., Yoshikawa, K., Zheleznyak, M., Lantuit, H., 2019. Permafrost is warming at a global scale. Nat. Commun. 10, 264. https://doi.org/10.1038/s41467-018-08240-4.

Blake, W.J., 1962. Geomorphology and Glacial Geology in Nordaustlandet, Spitsbergen. Unpublished PhD thesis. Department of Geology. Ohio State University, Columbus, p. 477.

Boulton, G.S., 1967. The development of a complex supraglacial moraine at the margin of Sørbreen, Ny Friesland, Vestspitsbergen. J. Glaciol. 47, 717–735.

Boulton, G.S., van der Meer, J.J.M., Beets, D.J., Hart, J.K., Ruegg, G.H.J., 1999. The sedimentary and structural evolution of a recent push moraine complex: Holmstrømbreen. Spitsbergen. Quat. Sci. Rev. 18, 339–371.

Bourriquen, M., Mercier, D., Baltzer, A., Fournier, J., Costa, S., Roussel, E., 2018. Paraglacial coasts responses to glacier retreat and associated shifts in river floodplains over decadal timescales (1966–2016), Kongsfjorden. Svalbard. Land Degrad. Dev. 29, 4173–4185.

Brückner, H., Schellman, G., 2003. Late Pleistocene and Holocene shorelines of Andréeland, Spitsbergen (Svalbard) – geomorphological evidence and paleo-oceanographic significance. J. Coast. Res. 19, 971–982.

Brynjólfsson, S., Schomacker, A., Ingólfsson, O., Keiding, J.K., 2015. Cosmogenic ^{36}Cl exposure ages reveal a 9.3 ka BP glacier advance and the Late Weichselian-Early Holocene glacial history of the Drangajökull region, northwest Iceland. Quat. Sci. Rev. 126, 140–157.

Burn, C.R., Smith, M.W., 1990. Development of thermokarst lakes during Holocene sites near Mayo. Yukon territory. Permafr. Periglac. Process. 1, 161–176.

Chandler, B.M.P., Lovell, H., Boston, C.M., Lukas, S., Barr, I.D., Benediktsson, Í.Ö., Benn, D.I., Clark, C.D., Darvill, C.M., Evans, D.J.A., Ewertowski, M.W., Loibl, D., Margold, M., Otto, J.-C., Roberts, D.H., Stokes, C.R., Storrar, R.D., Stroeven, A.P., 2018. Glacial geomorphological mapping: a review of approaches and frameworks for best practice. Earth Sci. Rev. 185, 806–846.

Christiansen, H.H., Humlum, O., Eckerstorfer, M., 2013. Central Svalbard 2000–2011 meteorological dynamics and periglacial landscape response. Arct. Antarct. Alp. Res. 43, 6–18.

Corbett, L.B., Bierman, P.R., Lasher, G.E., Rood, D.H., 2015. Landscape chronology and glacial history in Thule. northwest Greenland. Quat. Sci. Rev. 109, 57–67.

Cuffey, K.M., Conway, H., Gades, A.M., Hallet, B., Lorrain, R., Severinghaus, J.P., Steig, E.J., Vaugh, B., White, J.W.C., 2000. Entrainment at cold glacier beds. Geology 28, 351–354.

Dahlke, S., Hughes, N.E., Wagner, P.M., Gerland, S., Wawrzyniak, T., Ivanov, B., Maturilli, M., 2020. The observed recent surface air temperature development across Svalbard and concurring footprints in local sea ice cover. Int. Jour. Climatol. 40, 5246–5265. https://doi.org/10.1002/joc.6517.

Dallmann, W.K., 2015. Geoscience Atlas of Svalbard. Nor, 148. Polar Institute, Report Series, p. 292.

Donelly, R., Harris, C., 1989. Sedimentology and origin of deposits from a small ice-dammed lake, Leirbreen. Norway. Sedimentology 36, 581–600.

Dühnforth, M., Anderson, R.S., Ward, D., Stock, G.M., 2010. Bedrock fracture control of glacial erosion processes and rates. Geology 38, 423–426.

Eckerstorfer, M., Christiansen, H.H., Rubensdotter, L., Vogel, S., 2013. The geomorphological effect of cornice fall avalanches in the Longyeardalen valley, Svalbard. The Cryosphere 7, 1361–1374. https://doi.org/10.5194/tc-7-1361-2013.

Etzelmüller, B., Hagen, J.O., 2005. Glacier-permafrost interaction in Arctic and alpine mountain environments with examples from southern Norway and Svalbard. In: (eds) Harris, C., Murton, J.B.: Cryospheric Systems: Glaciers and Permafrost. Geological Society, London, Special Publications 242, 11–27.

Etzelmüller, B., Sollid, J.H., 1991. The role of weathering and pedological processes for the development of sorted circles on Kvadehuksletta, Svalbard – a short repor. Polar Res. 9, 181–191.

Evans, D.J.A., Strzelecki, M., Milledge, D.G., Orton, C., 2012. Hørbyebreen polythermal glacial landsystem. Svalbard. J. Maps 8, 146–156.

Ewertowski, M.W., Evans, D.J., Roberts, D.H., Tomczyk, A.M., 2016. Glacial geomorphology of the terrestrial margins of the tidewater glacier, Nordenskiöldbreen. Svalbard. J. Maps 12, 476–487.

Farnsworth, W.R., Ingólfsson, Ó., Retelle, M., Schomacker, A., 2016. Over 400 previously undocumented Svalbard surge-type glaciers identified. Geomorphology 264, 52–60. https://doi.org/10.1016/j.geomorph.2016.03.025.

Farnsworth, W.R., Ingolfsson, O., Noormets, R., Allaart, L., Alexanderson, H., Henriksen, M., Schomacker, A., 2017. Dynamic Holocene glacial history of St. Jonsfjorden, Svalbard. Boreas 46, 585–603.

Farnsworth, L.B., Kelly, M.A., Bromley, G.R.M., Axford, Y., Osterberg, E.C., Howley, J.A., Jackson, M.S., Zimmerman, S.R., 2018a. Holocene history of the Greenland Ice-Sheet margin in Northern Nunartarssuaq, Northwest Greenland. Arktos 4. doi:http://dx.doi.org/10.1007/s41063-018-0044-0.

Farnsworth, W.R., Ingolfsson, O., Retelle, M., Allaart, L., Håkansson, L.M., Schomacker, A., 2018b. Svalbard glaciers re-advanced during the Pleistocene–Holocene transition. Boreas 47, 1022–1032.

Farnsworth, W.R., Blake Jr., W., Guðmundsdottir, E.R., Ingólfsson, Ó., Kalliokoski, M.H., Larsen, G., Newton, A.J., Óladóttir, B.A., Schomacker, A., 2020a. Ocean-rafted pumice constrains postglacial relative sea-level and supports Holocene ice cap survival. Quat. Sci. Rev. 250, 106654.

Farnsworth, W.R., Ingolfsson, O., Alexanderson, H., Allaart, L., Forwick, M., Noormets, R., Retelle, M., Schomacker, A., 2020b. Holocene glacial history of Svalbard - status, perspectives and challenges. Earth Sci. Rev. 208, 103249.

Førland, E.J., Benestad, R., Hanssen-Bauer, I., Haugen, J.E., Skaugen, T.E., 2011. Temperature and precipitation development at Svalbard 1900–2100. Adv. Meteorol. 893790. https://doi.org/10.1155/2011/893790.

Forman, S.L., Lubinski, D.J., Ingólfsson, Ó., Zeeberg, J.J., Snyder, J.A., Siegert, M.J., Matishov, G.G., 2004. A review of postglacial emergence on Svalbard, Franz Josef Land and Novaya Zemlya. northern Eurasia. Quat. Sci. Rev. 23, 1391–1434.

French, F. (Ed.), 2018. The Periglacial Environment, 4th edition Wiley-Blackwell, Chichester, pp. 240–246.

Furrer, G., Stapfer, A., Glaser, U., 1991. Zur nacheiszeitlichen Gletschergeschichte des Liefdefjords (Spitzbergen)* (Ergebnisse der Geowissenschaftlichen Spitzbergenexpedition 1990). Geogr. Helv. 4, 147–155.

de Geer, G., 1896. Rapport om den svenska geologiska expeditionen till Isfjorden. på Spetsbergen sommaren 1896. Ymer 16, 259–266.

Gilbert, G.L., O'Neil, H.B., Nemec, W., Thiel, C., Christiansen, H.H., Buylaert, J-P, 2018. Late Quaternary sedimentation and permafrost development in a Svalbard fjord-valley, Norwegian high Arctic. Sedimentology 65, 2531–2558.

Gjerde, M., Bakke, J., D'Andrea, W.J., Balascio, N.L., Bradley, R.S., Vasskog, K., Ólafsdóttir, S., Røthe, T.O., Perren, B.B., Hormes, A., 2018. Holocene multi-proxy environmental reconstruction from Lake Hakluyvatnet, Amsterdamøya Island, Svalbard (79.5°N). Quat. Sci. Rev. 183, 164–176.

Gjermundsen, E.F., Briner, J.P., Akçar, N., Salvigsen, O., Kubik, P., Gantert, N., Hormes, A., 2013. Late Weichselian local ice dome configuration and chronology in Northwestern Svalbard: early thinning. late retreat. Quat. Sci. Rev. 72, 112–127.

Glasser, N.F., Hambrey, M.J., 2001. Styles of sedimentation beneath Svalbard valley glaciers under changing dynamic and thermal regimes. Journal of the Geological Society, London 158, 697–707.

Glasser, N.F., Kabbendam, M., 2011. Glacial erosion and bedrock properties in NW Scotland: abrasion and plucking. hardness and joint spacing. Geomorphology 130, 374–383.

Glasser, N.F., Crawford, K.R., Hambrey, M.J., Bennett, M.R., Huddart, B.D., 1998. Lithological and structural controls on the surface wear characteristics of glaciated metamorphic bedrock surfaces: Ossian Sarsfjellet. Svalbard. Jour. Geol. 106 (3), 319–330.

Glasser, N.F., Bennett, M.R., Huddart, D., 1999. Distribution of glaciofluvial sediment within and on the surface of a high Arctic valley glacier. Mathabreen, Svalbard. Earth Surf. Process. Landforms 24, 303–318.

Glasser, N.F., Roman, M., Holt, T.O., Žebre, M., Patton, H., Hubbard, A.L., 2020. Modification of bedrock surfaces by glacial abrasion and quarrying: evidence from North Wales. Geomorphology 365, 107283 https://doi.org/10.1016/j.geomorph.2020.107283.

de Haas, T., Kleinhans, M.G., Carbonneau, P.E., Rubensdotter, L., Hauber, E., 2015. Surface morphology of fans in the high-Arctic periglacial environment of Svalbard: controls and processes. Earth Sci. Rev. 146, 163–182.

Hagen, J.O., Liestøl, O., Roland, E., Jørgensen, T., 1993. Glacier Atlas of Svalbard and Jan Mayen. Norwegian Polar Institute, Oslo, pp. 1–167.

Hambrey, M.J., Huddart, D., Bennett, M.R., Glasser, N.F., 1997. Genesis of 'hummocky moraines' by thrusting in glacier ice: evidence from Svalbard and Britain. J. Geol. Soc. London 154, 623–632.

Hanáček, M., Flašar, J., Nývlt, D., 2011. Sedimentary petrological characteristics of lateral and frontal moraine and proglacial glaciofluvial sediments of Bertilbreen, Central Svalbard. Czech Polar Reports 1, 11–33.

Hanssen-Bauer, I., Forland, E.J., Hisdal, H., Mayer, S., Sando, A.B., Sorteberg, A., 2019. Climate in Svalbard 2100. Norwegian Centre for Climate Services Reports. Climate Services (NCCS), The Norwegian Centre for http://bora.uib.no/handle/1956/19136.

Harris, C., Kem-Luetschg, M., Christiansen, H.H., Smith, F., 2011. The role of interannual climate variability in controlling solifluction processes, Endalen. Svalbard. Permafr. Periglac. Process. 22, 239–253.

Hart, J.K., Watts, R.J., 1997. A comparison of the styles of deformation associated with two recent push moraines, south Van Keulenfjorden. Svalbard. Earth Surf. Process. Landf. 22, 1089–1107.

Hormes, A., Akcar, N., Kubik, P.W., 2011. Cosmogenic radionuclide dating indicates ice-sheet configuration during MIS 2 on Nordaustlandet. Svalbard. Boreas 40, 636–649.

Hormes, A., Gjermundsen, E.F., Rasmussen, T.L., 2013. From mountain top to the deep sea – deglaciation in 4D of the northwestern Barents Sea ice sheet. Quat. Sci. Rev. 75, 78–99.

Huddart, D., Hambrey, M.J., 1996. Sedimentary and tectonic development of a high-arctic thrust-moraine complex: Comfortlessbreen. Svalbard. Boreas 25, 227–243.

Humlum, O., 2005. Holocene permafrost aggradation in Svalbard. In: Harris, C., Murton, J. B. (Eds.), Cryospheric Systems: Glaciers and Permafrost. Geological Society, London, pp. 119–130 Special Publication, p. 242.

Humlum, O., Instanes, A., Sollid, J.L., 2003. Permafrost in Svalbard: a review of research history, climatic background and engineering challenges. Polar Research 22, 191–215.

Humlum, O., Elberling, B., Hormes, A., Fjordheim, K., Hansen, O.H., Heinemeier, J., 2005. Late-Holocene glacier growth in Svalbard, documented by subglacial relict vegetation and living soil microbes. The Holocene 15, 396–407.

Humlum, O., Christiansen, H.H., Juliussen, H., 2007. Avalanche-derived rock glaciers in Svalbard. Permafr. Periglac. Process. 18, 75–88.

Ingólfsson, Ó., 2011. Fingerprints of Quaternary glaciations on Svalbard. Geological Society of London, Special Publications 354, 15–31.
Ingólfsson, Ó., Rögnvaldsson, F., Bergsten, H., Hedenäs, L., Lemdahl, G., Lirio, J.M., Sejrup, H.P., 1995. Late Quaternary glacial and environmental history of Kongsøya. Svalbard. Polar Res. 14, 123–139.
Jonsson, S., 1983. On the geomorphology and past glaciation of Storöya. Svalbard. Geogr. Ann. 65A, 1–17.
Karczewski, A., Borowka, M., Gonera, P., Kasprzak, L., Kłysz, P., Kostrzewski, A., Lindner, L., Marks, L., Rygielski, W., Stankowski, W., 1990. Geomorphology-Petuniabukta Billefjorden Spitsbergen 1: 40 000. Adam Mickiewicz University, Poznań.
Kasprzak, M., Strzelecki, M.C., Traczyk, A., Kondracka, M., Lim, M., Migała, K., 2017. On the potential for a bottom active layer below coastal permafrost: the impact of seawater on permafrost degradation imaged by electrical resistivity tomography (Hornsund, SW Spitsbergen). Geomorphology 293, 347–359.
Kaufman, D.S., Ager, T.A., Anderson, N.J., Anderson, P.M., Andrews, P.M., Bartlein, P.J., Brubaker, L.B., Coats, L.L., Cwynar, L.C., Duvall, M.L., Dyke, A.S., Edwards, M.E., Eisner, W.R., Gajewski, K., Geirsdóttir, A., Hu, F.S., Jennings, A.E., Kaplan, M.R., Kerwin, M.W., Lozhkin, A.V., MacDonald, G.M., Miller, G.H., Mock, C.J., Oswald, W.W., Otto-Bliesner, B.L., Porinchu, D.F., Rühland, K., Smol, J.P., Steig, E.J., Wolfe, B.B., 2004. Holocene thermal maximum in the western Arctic (0–180°W). Quat. Sci. Rev. 23, 529–560.
Kaufman, D.S., Schneider, D.P., McKay, N.P., Ammann, C.M., Bradley, R.S., Briffa, K.R., Miller, G.H., Otto-Bliesner, B.L., Overpeck, J.T., Vinther, B.M., Arctic Lakes 2k Project Members., 2009. Recent warming reverses long-term arctic cooling. Science 325, 1236–1239.
Kavan, J., 2019. Post-little ice age development of coast in the locality of Kapp Napier, Central Spitsbergen, Svalbard Archipelago. Mar. Geodesy https://doi.org/10.1080/01490419.2019.1674429T.
Kjellman, S.E., Schomacker, A., Thomas, E.K., Håkansson, L., Duboscq, S., Cluett, A.A., Farnsworth, W.R., Allaart, L., Cowling, O.C., McKay, N.P., Brynjólfsson, S., Ingolfsson, O., 2020. Holocene precipitation seasonality in northern Svalbard: influence of sea ice and regional ocean surface conditions. Quat. Sci. Rev. 240, 1–15. https://doi.org/10.1016/j.quascirev.2020.106388, 106388.
Kelly, M.H., Anders, A.M., Mitchell, S.G., 2014. Influence of bedding dip on glacial erosional landforms, Uinta Mountains, USA. GFF, 147–159 https://doi.org/10.1111/geoa.12037.
Kleman, J., 1990. On the use of glacial striae for reconstruction of paleo-ice sheet flow patterns. Geogr. Ann. Series A. Phys. Geogr. 217–236.
Kleman, J., 1994. Preservation of landforms under ice sheets and ice caps. Geomorphology 9, 19–32.
Kristiansen, K.J., Sollid, J.L., 1986. Svalbard, glacial–geological and geomorphological map 1:1,000,000, map 2.3.5. National Atlas of Norway.
Landvik, J.Y., Bondevik, S., Elverhøi, A., Fjeldskaar, W., Mangerud, J., Salvigsen, O., Siegert, M.J., Svendsen, J.-I., Vorren, T.O., 1998. The last glacial maximum of Svalbard and the Barents Sea area: ice sheet extent and configuration. Quat. Sci. Rev. 17, 43–75.
Lantuit, H., Overduin, P.P., Couture, N., Wetterich, S., Aré, F., Atkinson, D., Brown, J., Cherkashov, G., Drozdov, D., Forbes, D.L., Graves-Gaylord, A., Grigoriev, M., Hubberten, H.-W., Jordan, J., Jorgenson, T., Ødegård, R.S., Ogorodov, S., Pollard, W.H., Rachold, V., Sedenko, S., Solomon, S., Steenhuisen, F., Streletskaya, I., Vasiliev, A., 2012. The Arctic coastal dynamics database: a new classification scheme and statistics on Arctic Permafrost Coastlines. Estuar. Coast. 35, 383–400.
Larsen, N.K., Piotrowski, J.A., Christoffersen, P., Menzies, J., 2005. Formation and deformation of basal till during a glacier surge; Elisebreen. Svalbard. Geomorphology 81, 217–234.
Larsen, E.A., Lysa, A., Rubensdotter, L., Farnsworth, W.R., Jensen, M., Nadeau, M.J., Ottesen, D., 2018. Late-glacial and Holocene glacier activity in the van Mijenfjorden area, western Svalbard. Arktos 4, 9. https://doi.org/10.1007/s41063-018-0042-2.
Liestøl, O., 1993. Glaciers of Svalbard, Norway. US Geological Survey Professional Paper 1386, E127–E151.
Lønne, I., 2005. Faint traces of high Arctic glaciations: an early Holocene ice-front fluctuation in Bolterdalen. Svalbard. Boreas 34, 308–323.
Lønne, I., 2016. A new concept for glacial geological investigations of surges, based on High-Arctic examples (Svalbard). Quat. Sci. Rev. 132, 74–100.
Lønne, I., Nemec, W., 2004. High-arctic fan delta recording deglaciation and environment disequilibrium. Sedimentology 51, 553–589.
Lovell, H., Boston, C.M., 2017. Glaciotectonic composite ridge system and surge-type glaciers: an updated correlation based on Svalbard, Norway. Arktos 3, 1–16 https://doi.org/10.1007/s41063-017-0028-5.
Lovell, H., Fleming, E.J., Benn, D.I., Hubbard, B., Lukas, S., Rea, B.R., Noormets, R., Flink, A.E., 2015. Debris entrainment and landform genesis during tidewater glacier surges. J. Geophys. Res. Earth Surf. 120, 1574–1595.
Lovell, H., Benn, D.I., Lukas, S., Ottesen, D., Luckman, A., Hardiman, M., Barr, I.D., Boston, C.M., Sevestre, H., 2018. Multiple Late Holocene surges of a High-Arctic tidewater glacier system in Svalbard. Quat. Sci. Rev. 201, 162–185.
Lyså, A., Larsen, E.A., Høgaas, F., Jensen, M.A., Klug, M., Rubensdotter, L., Szczuciński, W., 2018. A temporary glacier-surge ice-dammed lake, Braganzavågen. Svalbard. Boreas 47, 837–854.
Martín-Moreno, R., Álvarez, A., Hagen, J.O., 2017. 'Little Ice Age' glacier extent and subsequent retreat in Svalbard archipelago. The Holocene 27, 1379–1390.
van der Meer, J.J., 2004. Spitsbergen push moraines: including a translation of K. Gripp: Glaciologische und Geologische Ergebnisse Der Hamburgischen Spitzbergen-Expedition 1927. Elsevier, London 200 pp.
Meier, M.F., Post, A., 1969. What are glacier surges? Can. J. Earth Sci. 6, 807–817.
MET Norway, 2020. Norwegian Meteorological Institute. Data retrieved from https://sios-svalbard.org/results/?page=1 (accessed 29.01.2020).
Miccadei, E., Piacentini, T., Berti, C., 2016. Geomorphological features of the Kongsfjorden area: Ny-Ålesund, Blomstrandøya (NW Svalbard, Norway). Rendiconti Lincei 27, 217–228.
Nicu, I.C., Stalsberg, K., Rubensdotter, L., Martens, V.V., Flyen, A-C., 2020. Coastal Erosion Affecting Cultural Heritage in Svalbard. A Case Study in Hiorthhamn (Adventfjorden) – An Abandoned Mining Settlement. Sustainability 12, 2306; doi:https://doi.org/10.3390/su12062306.
Norwegian Polar Institute, 2019. SvalbardKartet. Fauna & Flora – Biogeographical Zones. Retrieved from. https://svalbardkartet.npolar.no/.
Nuth, C., Kohler, J., König, M., von Deschwanden, A., Hagen, J.O., Kääb, A., Moholdt, G., Petterson, R., 2013. Decadal changes from a multi-temporal glacier inventory of Svalbard. The Cryosphere 7, 1603–1621.
Österholm, H., 1990. The Late Weichselian Glaciation and Holocene shore displacement on Prins Oscars Land, Nordaustlandet, Svalbard. Geografiska Annaler Series A 72, 301–317.
Rouyet, L., Lauknes, T.R., Christiansen, H.H., Strand, S.M., Larsen, Y., 2019. Seasonal dynamics of a permafrost landscape, Adventdalen, Svalbard, investigated by InSAR. Remote Sens. Environ. 231, 111236. https://doi.org/10.1016/j.rse.2019.111236.
Rowland, J.C., Jones, C.E., Altmann, G., Bryan, R., Crosby, B.T., Hinzman, L.D., Kane, D.L., Lawrence, D.M., Mancio, A., Marsh, P., McNamara, J.P., Romanovsky, V.E., Toniolo, H., Travis, B.J., Trochim, E., Wilson, C.J., Geernaert, G.L., 2011. Arctic landscapes in transition: responses to thawing permafrost. Eos 91, 229–236.
Rubensdotter, L., Stalsberg, K., Christiansen, H., Eckersdorfer, M., Trøyen, P., 2015a. Landforms and sediments in Todalen and upper Gangdalen and Bødalen, Svalbard. Scale 1: 25,000. Norway, Geological Survey of.
Rubensdotter, L., Romundset, A., Farnsworth, F., Christiansen, H., 2015b. Landforms and sediments in Bjørndalen – Vestpynten, Svalbard. Quaternary Geological Map 1: 10,000. Norway, Geological Survey of.
Rubensdotter, L., Larsen, E., Lyså, A., 2016. Kvartærgeologisk og geomorfologisk kart Svea, Svalbard/Quaternary geological and geomorphological map, Svea, Svalbard. M 1: 15,000. Norway, Geological Survey of.
Salvigsen, O., 1978. Holocene emergence and finds of pumice, whalebones, and driftwood at Svartknausflya, Nordaustlandet. Norsk Polarinstitutt, Årbok 1977, 217–228.
Salvigsen, O., Österholm, H., 1982. Radiocarbon dated raised beaches and glacial history of the northern coast of Spitsbergen. Svalbard. Polar Res. 1, 97–115.
Schomacker, A., Kjær, K.H., 2008. Quantification of dead-ice melting in ice-cored moraines at the high-Arctic glacier Holmströmbreen. Svalbard. Boreas 37, 211–225.
Sessford, E.G., Bæverford, M.G., Hormes, A., 2015. Terrestrial processes affecting unlithified coastal erosion disparities in central fjords of Svalbard. Polar Res. 34, 24122. https://doi.org/10.3402/polar.v34.24122.
Sevestre, H., Benn, D.I., 2015. Climatic and geometric controls on the global distribution of surge-type glaciers: implications for unifying model of surging. J. Glaciol. 61, 646–662.
Sharp, M., 1988. Surging glaciers: behaviour and mechanisms. Prog. Phys. Geogr. 12, 349–370.
Siewert, M.B., Krautblatter, M., Christiansen, H.H., Eckerstorfer, M., 2012. Arctic Rockwall retreat rates estimated using laboratory-calibrated ERT measurements of talus cones in Longyeardalen, Svalbard. Earth. Surf. Proc. Land. 37, 1542–1555. https://doi.org/10.1002/esp.3297 2012.
Strand, S.M., Christiansen, H.H., Johansson, M., Åkerman, J., Humlum., 2020. Active layer thickening and controls on interannual variability in the Nordic Arctic compared to the circum-Arctic. Permafr. Periglac. Process., 1–12. https://doi.org/10.1002/ppp.2088.
Stroeven, A., Hättestrand, C., Jansson, K., Kleman, J., 2021. Paleoglaciology. In: Fowler, A., Ng, F. (Eds.), Glaciers and Ice Sheets in the Climate System. Springer Textbooks in Earth Sciences, geography and Environment. Springer, Cham , pp. 431–457. https://doi.org/10.1007/978-3-030-42584-5_17.
Strzelecki, M.C., Szczuciński, W., Dominiczak, A., Zagórski, P., Dudek, J., Knight, J., 2020. New fjords, new coasts, new landscapes: the geomorphology of paraglacial coasts formed after recent glacier retreat in Brepollen (Hornsund, southern Svalbard). Earth Surf. Process. Landforms 45, 1325–1334.
Szczęsny, R., Dzierżek, J., Harasimiuk, M., Nitychoruk, J., Pękala, K., Repelewska-Pękalowa, J., 1989. Photogeological Map of the Renardbreen, Scottbreen and Blomlibreen Forefield, (Wedel Jarlsberg Land, Spitsbergen), 1:10,000. Wydawnictwa Geologiczne, Warszawa.
Thompson, H.R., 1953. Geology and geomorphology in southern Nordaustlandet (North-East Land). Proceedings of the Geologists' Association 64, 293–312.
Tolgensbakk, J., 1990. Gipsdalen, Svalbard, Quaternary Geology and Geomorphology 1: 40,000. University of Oslo. Norwegian Polar Institute, Department of Physical Geography.
Tolgensbakk, J., Sørbel, L., & Høgvard, K. (2001). Geomorphological and Quaternary geological map of Svalbard 1: 100,000. Sheet C9Q Adventdalen. Map. Norw. Polar Inst. Temakart 31, 32.
Tomczyk, A.M., Ewertowski, M.W., Stawska, M., Rachlewicz, G., 2019. Detailed alluvial fan geomorphology in a high-arctic periglacial environment, Svalbard: application of unmanned aerial vehicle (UAV) surveys. J. Maps 15, 460–473.
Werner, A., 1993. Holocene moraine chronology, Spitsbergen, Svalbard: lichenometric evidence for multiple neoglacial advances in the Arctic. The Holocene 3, 128–137.
Witt-Nilsson, P., Gee, D.G., Hellman, F.J., 1998. Tectonostratigraphy of the Caledonian Atomfjella antiform of northern Ny-Friesland. Svalbard. Norsk Geologisk Tidsskrift 78, 67–80.
Zwoliński, Z., Giżejewski, J., Karczewski, A., Kasprzak, M., Lankauf, K.R., Migoń, P., Pękala, K., Repelewska-Pękalowa, J., Rachlewicz, G., Sobota, I., Stankowski, W., Zagórski, P., 2013. Geomorphological settings of Polish research areas on Spitsbergen. Landf. Anal. 22, 125–143.